

**Humoral responses induced by an
enzymatically active, whole-cell killed
pneumococcal vaccine**



Zoe Laan, B. Sc. (Biomedical Science)

A thesis submitted for the fulfilment of the
Degree of Master of Philosophy

School of Biological Sciences
The University of Adelaide
Adelaide, South Australia, Australia

January 2020

TABLE OF CONTENTS

LIST OF FIGURES AND TABLES.....	v
ABBREVIATIONS.....	vi
DECLARATION.....	xi
ACKNOWLEDGEMENTS.....	xii
PRESENTATIONS.....	xiv
ABSTRACT.....	xv
CHAPTER 1: LITERATURE REVIEW.....	1
1.1. <i>Streptococcus pneumoniae</i>.....	2
1.1.1. Global burden and disease.....	2
1.1.2. Pathogenesis.....	3
1.2. Immune response to <i>S. pneumoniae</i>.....	5
1.2.1. Innate immunity.....	5
1.2.2. Adaptive immunity.....	8
Cellular immunity.....	8
Humoral immunity and the role of the anti-protein antibody response.....	9
1.3. Treatment of pneumococcal disease.....	12
1.4. Pneumococcal vaccines.....	13
1.4.1. Purified polysaccharide vaccine (PPV).....	13
1.4.2. Protein conjugate vaccine (PCV).....	14
1.4.3. Serotype replacement.....	15
1.5. Experimental vaccines.....	16
1.5.1. Protein-based vaccines.....	16
1.5.2. Whole-cell inactivated vaccines.....	17
chemically inactivated pneumococcal vaccines.....	17
Gamma-irradiated pneumococcal vaccines.....	18
1.6. Project rationale.....	20
1.6.1. Hypothesis and aims.....	22
CHAPTER 2: MATERIALS AND METHODS.....	23
2.1. Ethics statement.....	24
2.2. Growing bacterial stocks.....	24
2.3. Neuraminidase assay.....	24
2.4. RNA extraction and qRT-PCR.....	25
2.5. Glucose utilisation assay.....	26

2.6. Generating serum.....	26
2.7. Enzyme-linked immunosorbent assay (ELISA).....	26
2.8. Flow cytometry.....	27
2.9. LRR fixation and capsule transmission electron microscopy (TEM).....	27
2.10. Uronic acid capsule quantification.....	28
2.11. Western blotting.....	29
2.12. Coomassie staining.....	29
2.13. Statistical analysis.....	30
CHAPTER 3: RESULTS.....	31
3.1. The enzymatic activity of gamma-irradiated <i>S. pneumoniae</i>.....	32
3.1.1. Retention of enzymatic activity by inactivated pneumococci.....	32
3.1.2. RNA expression by irradiated pneumococci.....	33
3.1.3. Glucose utilisation as an indicator of broad-spectrum metabolic activity.....	34
3.2. Humoral responses induced by γ-PN(ΔPsaA) and their interactions with encapsulated strains of <i>S. pneumoniae</i>.....	34
3.2.1. Cross-reactivity of γ -PN(Δ PsaA)-induced antibodies against different pneumococcal serotypes.....	35
3.2.2. The effect of growth medium on capsule expression.....	36
3.2.3. Antibody binding to encapsulated serotype 2 (strain D39).....	38
3.2.4. The effect of vaccination route on IgG subclass profiles.....	39
3.2.5. Antibody binding to encapsulated serotype 3.....	39
CHAPTER 4: DISCUSSION.....	55
4.1. Characterisation of gamma-irradiated pneumococci.....	56
4.2. Interactions between γ -PN(Δ PsaA)-induced antibodies and encapsulated strains of pneumococci.....	59
4.3. Future directions.....	63
4.4. Conclusion.....	64
CHAPTER 5: REFERENCES.....	67

LIST OF FIGURES AND TABLES

Table 2.1	Primers used for qRT-PCR experiments
Figure 3.1	Neuraminidase activity of pneumococci inactivated using different mechanisms
Figure 3.2	qRT-PCR of inducible genes controlled by the raffinose and galactose operons under inducing and non-inducing conditions.
Figure 3.3	Glucose utilisation by live (0kGy) and irradiated (16kGy) pneumococci.
Figure 3.4	Western blot (A) and Coomassie stain (B) of whole-cell lysates from PCV (A.1, B.1) and non-PCV serotypes (A.2, B.2).
Figure 3.5	Transmission electron microscopy (TEM) of serotype 2 (strain D39) pneumococci grown in different mediums.
Figure 3.6	Measurements of capsule thickness (A) and total capsular polysaccharide (CPS) production (B) by serotype 2 pneumococci.
Figure 3.7	Transmission electron microscopy (TEM) of serotype 3 pneumococci grown in different mediums.
Figure 3.8	Measurements of capsule thickness (A) and total capsular polysaccharide (CPS) production (B) by serotype 3 pneumococci.
Figure 3.9	IgG binding to serotype 2 pneumococcal cells grown in different mediums and treated with serum from mice vaccinated via IP route.
Figure 3.10	IgG binding to serotype 2 pneumococcal cells grown in different mediums and treated with serum from mice vaccinated via IM using alum as adjuvant.
Figure 3.11	The effect of vaccination route and adjuvant on IgG subclass profiles.
Figure 3.12	IgG binding to serotype 3 pneumococcal cells grown in different mediums and treated with serum from mice vaccinated via IP route.
Figure 3.13	IgG binding to serotype 3 pneumococcal cells grown in different mediums and treated with serum from mice vaccinated via IM route with alum adjuvant.

ABBREVIATIONS

Δ/δ	Delta
γ	Gamma
γ -PN	Gamma-irradiated pneumococcal vaccine
ABC	ATP-binding cassette
AEC	Animal Ethics Committee
ANOVA	Analysis of variance
ANSTO	Australia's Nuclear Science and Technology Organisation
AOM	Acute otitis media
BPL	β -propiolactone
BBB	Blood-brain barrier
BCA	Bicinchoninic acid
BSA	Bovine serum albumin
C1q	Complement component 1q
CbpA	Choline binding protein A
CD4/8	Cluster of differentiation 4/8
CFU	Colony forming units
^{60}Co	Cobalt-60
CpG	5' – cytosine – phosphate – guanine– 3'
CPS	Capsular polysaccharide
CRP	C-reactive protein
CTL	Cytotoxic T lymphocyte
$^{\circ}\text{C}$	Degrees Celsius
DEPC	Diethyl pyrocarbonate
DNA	Deoxyribonucleic acid
DOC	Deoxycholate
ELISA	Enzyme-linked immunosorbent assay
EndA	Endonuclease A
EtOH	Ethanol

Fc	Fragment crystallisable
F and R primers	Forward and reverse primers
f.s	Filter sterilised
g	Grams
GlcNAc	N-acetyl-glucosamine
GMFI	Geometric mean fluorescence intensity
GMP	Good manufacturing practice
³ H	Tritium
HI	Heat inactivated
HIV	Human immunodeficiency virus
H+L	Heavy and light chain
HRP	Horse radish peroxidase
H ₂ SO ₄ /Na ₂ BO ₄	Sulfuric/sodium tetraborate
IFN-	Interferon
Ig	Immunoglobulin
IL-	Interleukin
IM	Intramuscular
IP	Intraperitoneally
IPD	Invasive pneumococcal disease
IVIG	Human intravenous immunoglobulin
KBMA	Killed but metabolically active
kDa	Kilodalton
kGy	KiloGray
LRR	Lysine ruthenium red
LytA	Autolysin
M	Molar
mA	Milliamperes
µg	Microgram
MES	2-(<i>N</i> -morpholino)ethanesulfonic acid
mg	Milligram
MgSO ₄	Magnesium sulphate

MHC	Major histocompatibility complex
MIP-2	Macrophage inflammatory protein 2
μl	Microliter
ml	Millilitre
mM	Millimolar
Mn ²⁺	Manganese (II)
mRNA	Messenger RNA
4-MU	4-methylumbelliferyl
4-MUNANA	4-methylumbelliferyl-N-acetyl-α-D-neuraminic acid
Na ₂ CO ₃	Sodium carbonate
NanA	Neuraminidase A
NANA	N-acetyl-α-D-neuraminic acid
NaOH	Sodium hydroxide
NDMA	Non-dividing but metabolically active
NET	Neutrophil extracellular trap
ng	Nanogram
NK	Natural killer cell
NLRP3	NOD- LRR- pyrin domain-containing protein 3
nm	Nanometres
NSW	New South Wales
NT-Spn	Non-typeable <i>Streptococcus pneumoniae</i>
NVT	Non-vaccine serotype
OD ₆₀₀	Optical density at 600nm
OP(K)A	Opsonophagocytic (killing) activity
PAF	Platelet activating factor
PAF-R	Platelet activating factor receptor
PAMP	Pathogen associated molecular pattern
PBS	Phosphate buffered saline
PCR	Polymerase chain reaction
PCV	Protein conjugate vaccine

PdT	Pon-haemolytic pneumolysin mutant
PFA	Paraformaldehyde
pIgR	Polymeric Ig receptor
Ply	Pneumolysin
PPV	Purified polysaccharide vaccine
PRR	Pattern recognition receptor
PsaA	Pneumococcal surface adhesin A
PspA	Pneumococcal surface protein A
PspC	Pneumococcal surface protein C
qRT-PCR	Quantitative reverse transcription polymerase chain reaction
RCT	Randomised placebo-controlled trials
rcf	Relative centrifugal force
RFU	Relative fluorescence units
RNA	Ribonucleic acid
rpm	Rotations per minute
SDS	Sodium dodecyl sulphate
SDS-PAGE	Sodium dodecyl sulphate-polyacrylamide gel
SEM	Standard error of mean
SILAC	Stable isotope labelling by/with amino acids in cell culture
T _x	Time _{hours}
TCA	Trichloroacetic acid
TCR	T-cell receptor
TD	T-dependent
TEM	Transmission electron microscopy
Th	T helper
TI	T-independent
TLR	Toll-like receptor
TLR ^{-/-}	TLR double knock-out
TMB	Tetramethylbenzidine
TMP-SMX	Trimethoprim-sulphamethoxazole
TNF- α	Tumour necrosis factor alpha

UAA	Uronic acid assay/capsule quantification
US	United States
UV	Ultraviolet
V	Voltage
13/23v	13/23 valent
VEEV	Venezuelan Equine Encephalitis Virus
WCV	Whole-cell vaccine
w/v	Weight per volume

DECLARATION

I certify that this work contains no material which has been accepted for the award of any other degree or diploma in my name, in any university or other tertiary institution and, to the best of my knowledge and belief, contains no material previously published or written by another person, except where due reference has been made in the text. In addition, I certify that no part of this work will, in the future, be used in a submission in my name, for any other degree or diploma in any university or other tertiary institution without the prior approval of the University of Adelaide and where applicable, any partner institution responsible for the joint-award of this degree.

I acknowledge that copyright of published works contained within this thesis resides with the copyright holder(s) of those works.

I also give permission for the digital version of my thesis to be made available on the web, via the University's digital research repository, the Library Search and also through web search engines, unless permission has been granted by the University to restrict access for a period of time.

I acknowledge the support I have received for my research through the provision of an Australian Government Research Training Program Scholarship.

Zoe Laan

ACKNOWLEDGEMENTS

First and foremost, I would like to give my endless thanks to my principle supervisor, Dr. Mohammed Alsharifi. You have spent many hours with me over the past two years, always offering your guidance, patience, and understanding. You've not only taught me invaluable lessons in critical thinking and scientific practice, but you've shared with me experiences from your life and lessons you've learnt along the way that will stay with me forever. I cannot thank you enough for your support and for your belief in me.

I am also deeply thankful to my co-supervisor, Prof. James Paton. You have always found time to offer your advice and feedback, and your enthusiasm for good data has been infectious. I would also like to thank you for supporting my attendance at Europneumo, an experience that has helped to shape my confidence in both myself and my work, and allowed me to make memories that I couldn't have anywhere else.

I would also like to give a special mention to Prof. Tim Hirst. I always looked forward to your visits and the discussions in our group meetings. Thank you taking time out of your busy schedule to offer your advice and lend a different perspective to my experiments.

To Shannon; you have been with me every step of the way through this project. You inspire me every day with your passion, intelligence, and kindness. I will be forever grateful for the time and effort you invested in me both as a budding young scientist, and as a friend. To Eve; while we might have been working on different projects, you were always there to offer guidance in the lab and with data (especially maths). Thank you for the endless laughs, chats, and moral support. To Chloe; you may have been the newest to our lab, but it didn't feel that way after long. Our little lab wouldn't be the same without you now. Thank you for all of your encouragement and enthusiasm over the last year. I can't wait to see what each of you will achieve in the future.

I would also like to thank the members of the Paton Lab for their support. Thank you Vik and Claudia for helping me with experiments, Kim for your infectious smile and enthusiasm, and

Erin for your advice and company on our trip. I would also like to thank Austen for his guidance in animal work. A very special thank you to Cathy; thank you for all of your support of the team and in the lab – we would be lost without you!

Finally, I would like to thank Aidan. Your support, love, and encouragement have helped to keep me going over the last two years. Thank you for being my shoulder to lean on, for all the late-night hours we spent watching TV, and for all the coffee. I hope I'll be able to return the favour when its your turn.

PRESENTATIONS

CONFERENCE PRESENTATIONS		
Type	Title	Conference
Poster presentation	Gamma-irradiated pneumococci are replication incompetent but retain metabolic activities	14th European Meeting on the Molecular Biology of the Pneumococcus, Greifswald, Germany, June 2019

ABSTRACT

Streptococcus pneumoniae is a key pathogen of the human respiratory tract responsible for approximately one million deaths per year, the majority of which occur in young children in developing countries. Vaccination strategies against the pneumococcus currently target the dominant immunogen of the bacterium, the polysaccharide capsule. While this has proved highly effective against vaccine-included serotypes, serotype replacement has prevented continued reductions in rates of pneumococcal disease over the last two decades. In order to continue reducing the prevalence of pneumococcal disease, a novel, serotype-independent vaccination strategy is required. Our lab has previously described a new, gamma-irradiated pneumococcal vaccine termed γ -PN Δ PsaA. This vaccine contains a whole-cell, unencapsulated pneumococcal antigen inactivated using gamma-irradiation, and induces a serotype-independent immune response against highly conserved, sub-capsular protein antigens.

Gamma-irradiation inactivates micro-organisms primarily through direct damage to genetic material, introducing strand breakages and preventing genome replication. Unlike genetic material, proteins are more resistant to direct damage and remain intact throughout the irradiation process. Data from this study showed that irradiated pneumococci retain functional enzymes utilised for virulence and gene expression, and it was shown that some genes may be more susceptible to direct damage than others. Furthermore, irradiated pneumococci appear to be capable of responding to environmental signals by modifying gene expression accordingly. Despite retaining functional enzymes and transcriptional abilities, irradiated pneumococci do not appear to be capable of metabolising carbohydrates.

As the vast majority of pathogenic strains of pneumococci are encapsulated, it was essential to examine the functionality of γ -PN Δ PsaA-specific antibodies against encapsulated pneumococci. Immune serum was generated by vaccinating mice via different routes, and antibody binding to pneumococcal cells expressing various capsule phenotypes was assessed. It was shown that both capsule structure and IgG subclass profiles play a role in influencing

antibody binding against encapsulated pathogens. Of particular interest, it appears that certain IgG subclass profiles may be more effective at binding sub-capsular antigens on pneumococci expressing a wider variety of capsule phenotypes.

CHAPTER 1

Literature review

1.1. *Streptococcus pneumoniae*

Streptococcus pneumoniae (the pneumococcus) is an important pathogen of the human respiratory tract [1], associated with significant levels of global morbidity and mortality. The pneumococcus is a Gram-positive bacterium, with virulent strains typically expressing a polysaccharide capsule. To date, over 90 distinct capsular serotypes have been identified [2]. The pneumococcus is found as an asymptomatic coloniser of the nasopharynx in 5-30% of healthy adults and 10-50% of healthy children [3]. Colonising strains are generally cleared from the nasopharynx within 4 – 8 weeks [1], however, spread of colonising pneumococci from the nasopharynx to sterile sites can lead to the development of disease [4].

1.1.1. Global burden and disease

The pneumococcus has remained a key human pathogen since its identification in 1881. Historically, the pneumococcus has caused large scale mortality during events such as the 1918 Spanish influenza pandemic [5], and remains responsible for up to half of all cases of community-acquired pneumonia and otitis media [6]. In children less than 5 years old, pneumococcal diseases cause over 1 million deaths annually [7], with the majority of these deaths occurring in developing countries [8]. Key risk factors for the development of pneumococcal disease include age, with prevalence highest amongst children younger than 2 years old and adults over 65 years old, immunocompetence status, with HIV-positive children at a higher risk for developing IPD [9], co-infection with other respiratory pathogens such as influenza [10, 11], and genetic background [3].

S. pneumoniae is capable of causing a wide range of pathologies with varying severity. Milder forms of disease include acute otitis media (AOM), an infection of the middle ear, and sinusitis, in which the sinuses become inflamed. Life-threatening pathologies can arise upon the development of invasive pneumococcal diseases (IPDs) such as meningitis, an infection of the membranes surrounding the brain and spinal cord, and bacteraemia, occurring when bacteria enter the bloodstream [3, 12, 13]. Bacterial meningitis is one of the top ten global causes of death by infectious disease. In developed countries, community-acquired meningitis, in which

S. pneumoniae is the causative agent, has a case-fatality rate of approximately 20% [14]. Up to 40% of survivors suffer long-term effects including deafness and neurological disability [15]. The situation in developing countries is more severe, with a case-fatality rate of up to 50% and around 60% of survivors suffering long-term effects [16-18].

As previously mentioned, the pneumococcus is also a causative agent of pneumonia, the leading cause of pneumococcal death worldwide [19, 20]. *S. pneumoniae* has been implicated in up to two thirds of cases of community-acquired bacteraemic pneumonia [21] and is estimated to cause approximately 550,000 cases of pneumonia annually [22].

1.1.2. Pathogenesis

All cases of pneumococcal disease are preceded by nasopharyngeal colonisation. While the majority of individuals will clear a colonising serotype within weeks to months (depending on age), spread of the pneumococcus to sterile sites of the body leads to the development of disease, particularly in those belonging to at-risk groups mentioned earlier. Contact with infectious respiratory secretions allows for the dissemination of the pneumococcus throughout the population [23], with young children acting as carriage reservoirs. To successfully colonise a new host, the pneumococcus must make use of a vast array of virulence factors required for bacterial-host cell interactions and immune evasion.

Asymptomatic colonisation occurs when pneumococci adhere to resting cells of the respiratory epithelium in the nasopharynx. Surface proteins mediate adhesion directly through adhesin-receptor interactions, and indirectly by contributing to the hydrophobic and electrostatic surface characteristics of the pneumococcus, facilitating non-specific, physiochemical interactions between bacterial and host cells [13, 24]. Direct interactions typically occur between cell-wall associated protein adhesins, such as pneumococcal surface protein A (PspA) and other choline binding proteins [25, 26], and host-cell surface carbohydrates [23]. The pneumococcus is also capable of remodelling the host environment using enzymes such as neuraminidase A (NanA) to decrease the viscosity of mucous, reducing nasopharyngeal clearance. NanA also functions in the removal of terminal sugar residues from host

glycoconjugates, exposing receptors such as N-acetyl-glucosamine (GlcNAc) for the pneumococcus to bind to [23, 27]. Under pro-inflammatory conditions, another virulence factor, choline binding protein A (CbpA), interacts directly with host cell polymeric Ig receptor (pIgR), leading to internalisation and transcytosis of the pneumococcus across the epithelial barrier [28]. From here, bacterial dissemination to other niches can begin, along with the development of pneumococcal disease.

The polysaccharide capsule predominantly functions to enhance resistance to opsonophagocytosis, complement-mediated killing [29], and clearance at mucosal surfaces [30]. The capsule is made up of chains of repeating monosaccharide units decorated with various sidechains [31], whose organisation, exportation, and synthesis is determined by enzymes encoded by an array of *cps* genes [32]. More complex chain structures may possess acetylated sugars, and oligosaccharide repeat units may include phosphodiester linkages, pyruvate, and glycerol amongst other inclusions [33]. Serological differences between each serotype arise from the possession of different genes encoding highly substrate-specific glycosyltransferases responsible for forming glycosidic linkages between sugar moieties [34]. Polysaccharide chain length and capsule thickness are key points of structural variability between serotypes. Chain length has been linked to substrate availability during growth, for example, modulation of UDP-GlcUA and UDP-Glc availability has been shown to influence polysaccharide chain length, with UDP-GlcUA availability positively correlating with polysaccharide chain length in serotype 3 [35]. Capsule thickness is also associated with carbon source availability in vitro, for example, larger capsules are produced when glucose is the predominant carbon source, while thinner capsules are produced when fructose acts as the main carbon source [36].

Importantly, capsular serotype is intrinsically linked to both virulence and disease type, with up to 100-fold variability in invasiveness between different capsular serotypes. In fact, only 20-30 of the >90 identified serotypes in humans are routinely able to cause IPD [37, 38], due to differences in the ability of their capsule layer to evade host immune responses. This has been demonstrated by multiple studies using capsule switch pneumococcal mutants. For example, serotype 5 is highly virulent, though expressing a serotype 3 capsule in a serotype 5

genetic background generated a completely avirulent pneumococcal strain. Conversely, expressing serotype 3 capsule on a serotype 6 genetic background generated a switch mutant that was significantly more virulent than its wild-type parental strain. Furthermore, authors observed no significant difference in virulence when the serotype 3 capsule was expressed in a serotype 2 genetic background compared with the parental serotype 2 strain [39]. This study led to formulation of two distinct hypotheses as to why virulence may be so dramatically altered by capsule switching. Firstly, an interplay between specific capsule types and virulence factors may be required for virulence in wildtype strains, and secondly, changes in virulence associated with capsule switching may be due to changes in sub-capsular antigen shielding by different capsule types.

IPDs such as bacteraemia and meningitis involve the dissemination of the pneumococcus from the epithelium to the blood, and subsequently across the blood-brain barrier (BBB). To facilitate this movement, the pneumococcus hijacks aspects of the host's immune response under pro-inflammatory conditions [26]. Bacterial cell wall components and lipotechoic acids stimulate the release of pro-inflammatory cytokines IL-1, tumour necrosis factor (TNF)- α , and IL-12, generating an acute inflammatory response [40] to the disseminating pneumococci. In response, host cells upregulate surface molecules such as platelet activating factor receptor (PAF-R). PAF-R is the receptor for PAF, a lipid chemokine which enhances endothelial permeability and leukocyte extravasation to inflamed sites [41]. The pneumococcus capitalises on this, binding in place of PAF via a phosphorylcholine determinant of cell wall teichoic acid shared with PAF [42], undergoing transcytosis from the bloodstream into susceptible tissues to cause disease.

1.2. Immune response to *S. pneumoniae*

1.2.1. Innate immunity

The mucosal layer of the respiratory tract acts as the first innate barrier to pneumococcal infection, preventing direct access to the respiratory epithelium below and trapping pneumococcal cells. The ionic effects of the negatively-charged capsular polysaccharide aid

in avoiding mucosal entrapment by repelling sialic acid-rich mucopolysaccharides [30]. At the host cell surface, an array of pattern recognition receptors (PRRs) play a synergistic, although partially redundant, role in innate sensing of pneumococcal pathogen associated molecular patterns (PAMPs). This drives the initiation of pro-inflammatory responses and recruitment of phagocytes to mediate bacterial clearance, and subsequently guides the development of the adaptive immune response.

Toll-like receptor 2 (TLR2), located at the host cell surface, is a key innate sensor of Gram-positive bacteria [43], detecting cell wall components such as peptidoglycan, lipoteichoic acid, and lipoprotein [44]. TLR2 plays a role in inflammation following intranasal administration of pneumococcal lipoteichoic acid in mice, driving TLR2-dependent neutrophil influx, and production of cytokines TNF- α , IL-1 β , IL-6 and MIP-2 [45]. In murine models of pneumococcal pneumonia, TLR2 has been implicated in the early stages of inflammatory responses driven by alveolar macrophages [46]. In addition, TLR2 has been shown to play a protective role in meningitis, with TLR2^{-/-} mice demonstrating aggravated disease progression, reduced immune cell recruitment, and increased bacterial loads on the brain [47]. TLR4, another cell-surface TLR [43], has also been implicated as a key sensor and regulator of the innate immune response to the pneumococcus, with TLR4^{-/-} mice significantly more susceptible to lethal pneumococcal infection. Macrophages were found to mount a TLR4-mediated pro-inflammatory response to the pore-forming toxin, pneumolysin (Ply). This sensing capability is thought to occur via specific interactions between Ply and TLR4, rather than a sensing mechanism dependent on the cytotoxic effects of Ply, as non-toxic Ply also stimulates TLR4-mediated inflammatory responses [48]. Ply has also been shown to be a potent activator of the NLRP3 inflammasome, driving IL-1 β production in macrophages and dendritic cells in a TLR4-independent manner, with inflammasome activation playing an important role in bacterial clearance and maintenance of respiratory epithelial and endothelial barriers [49]. Unlike cell surface TLRs 2 and 4, TLR9, the endosomal TLR sensing unmethylated CpG dinucleotides, has been found to have a redundant role in models of nasopharyngeal colonisation and meningitis [50, 51]. TLR9 does, however, play a key role in driving early phagocytic uptake and killing of pneumococci in murine models of pneumonia [52].

In addition to TLRs, opsonophagocytic killing plays a key part in the innate immune response to *S. pneumoniae*. Alveolar macrophages act as first responders in the lungs and are capable of clearing low bacterial burdens. As larger numbers of pneumococci accumulate in the airways and inflammation persists, neutrophils are recruited and become the dominant phagocyte [23, 53]. The complement system acts as an integral part of bacterial opsonisation to enhance phagocytic killing, with the classical pathway playing the largest role [54]. The classical pathway was thought to be an exclusive arm of the adaptive immune response, activated by C1q protein binding to the Fc portion of specific IgG antibody-antigen complexes [55]. However, C1q has been shown to be capable of binding directly to bacterial surfaces [56], indirectly via association with natural IgM [57], and to C reactive protein (CRP) bound to bacterial phosphorylcholine [58]. The capsule plays a large role in innate immune evasion by reducing the deposition of complement activating factors, such as CRP, and opsonins such as C3b/iC3b, on the bacterial cell surface. The capsule extends its role to preventing adaptive IgG-mediated activation of the classical complement pathway by shielding sub-capsular antigens from recognition by antigen-specific IgG [59]. Opsonophagocytosis is further evaded through steric hinderance as the capsule prevents interactions between the Fc portions of bound antibodies and the Fc γ receptors of phagocytic cells [30, 60]. Additionally, neutrophils can mediate killing via the release of neutrophil extracellular traps (NETs) containing high levels of antimicrobial peptides in a DNA scaffold [61]. The pneumococcus possesses an endonuclease (endA) used to degrade the DNA scaffold of NETs, mediating escape and preventing bacterial killing [62]. Evasion of natural antibody responses at the mucosal surface is also conferred by enzymatic virulence factors such as IgA protease, which cleave the protease sensitive hinge region of IgA, the dominant immunoglobulin of the human respiratory tract [63].

$\gamma\delta$ T cells, a subset of lymphocytes associated with the innate immune response, are also essential for early host defences against pneumococcal infection. TCR-V γ 4^{-/-} mice exhibit significantly higher bacterial loads and reduced neutrophil influx into the lungs, ultimately leading to reduced survival, demonstrating an essential role for tissue-specific subsets of $\gamma\delta$ T cells in pulmonary clearance of pneumococci [64]. Importantly, $\gamma\delta$ T cells have been

demonstrated to be key producers of IL-17 in response to *Mycobacterium tuberculosis* infection [65], and thus may also participate in anti-pneumococcal immune responses as producers of IL-17. In fact, intranasal vaccination of mice with a whole-cell, gamma-irradiated pneumococcal vaccine has previously been demonstrated to induce innate IL-17 responses [66]. This cytokine plays a key role in coordinating localised inflammatory responses through the induction of pro-inflammatory cytokine expression and neutrophil recruitment and activation [67].

1.2.2. Adaptive immunity

Acquired pneumococcal immunity depends on both cellular and humoral immune responses to effectively prevent colonisation and disease. Each episode of pneumococcal carriage acts as an immunising event against the carriage serotype, leading to subsequent increases in immunity to the pneumococcus in serotype-dependent and –independent manners.

Cellular immunity

The essential role for CD4+ T cells in protection against pneumococcal disease is highlighted by rates of pneumococcal disease in HIV+ individuals. HIV infection in adults is associated with a 50-fold increased risk of developing pneumococcal disease and reduced colonisation-free periods [68, 69]. A study in μ MT and MHCII^{-/-} mice found that both antibody- and CD4+ T cell-mediated responses were involved in protection against mucosal colonisation and the development of IPD [70]. Subsequent studies aimed to elucidate which cytokines and T helper cell subsets were responsible for adaptive immunity to the pneumococcus following colonisation. IFN- γ , IL-4, and IL-17AR knockout mice were immunised with a whole-cell vaccine (WCV) preparation (previously shown to induce CD4+ T cell-dependent protection [71]) and protection against colonisation was assessed. It was revealed that naïve and vaccinated IL-17AR knockout mice were highly susceptible to pneumococcal colonisation, indicating a crucial role for IL-17A in the secondary immune response [72]. Further investigation supported the role of IL-17A in late stage clearance of pneumococcal colonisation via monocyte/macrophage recruitment in a TLR2-, CD4+ T cell-, and IL-17A-

dependent manner. TLR2^{-/-} and CD4⁺ T or IL-17A cell depleted mice showed delayed late stage clearance of colonising pneumococci during primary exposure, with reduced recruitment of monocytes and macrophages to facilitate clearance. Depletion of CD4⁺ T cells and IL-17A at the time of secondary challenge also abolished enhanced early clearance via phagocyte recruitment, further highlighting the key role of IL-17A producing T helper cell subsets in both primary and secondary immune responses [73].

IL-17 has also been implicated in human responses to the pneumococcus. In a model of experimental human carriage, nasopharyngeal pneumococcal colonisation was associated with the expansion of pneumococcal-specific IL-17⁺ CD4⁺ (Th17) effector and memory T cell populations in the lung [74]. Furthermore, those carrying polymorphisms in the IL-17A gene, *IL17A*, are more susceptible to colonisation and lung infection by Gram-positive bacteria [75, 76].

The protective effects of Th17 responses in mice have also been shown to be synergistic with antibody responses, enhancing phagocytic capabilities in the lung through increased phagocyte recruitment and enhanced leakage of anti-pneumococcal IgG from the serum into the lung, increasing bacterial opsonisation [77].

Humoral immunity and the role of the anti-protein antibody response

As *S. pneumoniae* is predominantly an extracellular pathogen, opsonising antibodies are essential for the effective clearance of pneumococci via opsonophagocytic methods described earlier. Protective antibody responses to the pneumococcus were thought to be primarily driven by the development of serotype-specific anti-capsular antibodies, however, recent data has begun to challenge this paradigm, highlighting a role for the anti-protein antibody response in protection against pneumococcal disease.

The key role of systemic antibody responses has been highlighted in a murine model of pneumonia and subsequent bacteraemia. μ MT mice lacking antibody responses rapidly develop bacteraemia upon challenge, however, passive transfer of anti-pneumococcal

antibodies from serum isolated from vaccinated mice greatly reduced bacterial burden in the lungs and the likelihood of developing bacteraemia. Furthermore, serum from colonised mice enhanced neutrophil-mediated phagocytosis, compared with serum from uncolonised or μ MT mice [78]. However, this study did not distinguish between IgG directed against capsular polysaccharide and protein antigens. Interestingly, a previous study indicated partial antigenic redundancy between pneumococcal antigenic groups, with unencapsulated mutants also inducing protective antibody responses in mice [79].

In general, Ig isotype and subclass profiles have been demonstrated to be dependent on the inducing antigen. In mice, capsule specific antibody responses are typically dominated by IgM and IgG3, while protein specific responses are dominated by IgG2b and IgG2a [80]. In humans, antibody responses to carbohydrate antigens are typically dominated by IgG2, followed by IgG1, while anti-protein responses are dominated by IgG1 and IgG4 [81]. IgG1, rather than IgG2, is a more effective opsonin and activator of the classical complement pathway, the main complement pathway involved in anti-pneumococcal responses. Interestingly, IgG1:IgG2 ratios have been found to vary between age groups, with IgG2 typically higher in adults, and IgG1 dominant in infants in response to polysaccharide antigen [82, 83]. The effect of IgG1:IgG2 ratios has been found to have a negative, though non-significant, impact on opsonophagocytic activity (OPA) *in vitro*, with total anti-capsule IgG titres playing a more significant role in OPA [82].

Despite the association between anti-capsular IgG and *in vitro* OPA, human intravenous immunoglobulin (IVIG) depleted of anti-capsular IgG was demonstrated to retain agglutinating capabilities against encapsulated pneumococci [84]. Furthermore, depleted IVIG has been shown to prevent the development of IPD in mouse models, demonstrating a clear protective role for antibodies targeting non-polysaccharide antigens [84].

Further compelling evidence for the role played by anti-protein, rather than anti-capsular, antibodies in natural immunity to *S. pneumoniae* arises from analysis of IgG titre kinetics and age-related declines in pneumococcal disease. Incidence of pneumococcal disease follows a well-known trend; peaking in infancy, declining significantly in children over 5 years old and

adults, and rising again in the elderly [85]. Assuming anti-capsular antibodies are primarily responsible for age related declines in IPD, it would be expected that anti-capsular antibody titres would increase significantly over the first few years of life. In a study examining IgG responses to pneumococcal antigens in infants, it was found that between 5.6% and 85.7% of infants developed serum IgG concentrations above the putative protection level for IPD (0.35mg/L) in a serotype-specific manner. Considering this high level of variability, it is unlikely that serotype-specific anti-capsular IgG is contributing to the serotype-independent phenomenon of age-related decline in IPD [86]. Comparatively, a number of studies have observed rapid increases in IgG levels against protein antigens over the first two years of life. Unlike capsular polysaccharide, the antigenic structure of pneumococcal proteins is highly conserved between serotypes.

Studies of anti-protein antigen titres in different age groups in Kenya found that anti-pneumolysin titres increased four-fold over the first years of life, reaching adult titres by four years of age, while anti-PspA IgG titres increased 13-fold over the same time period. Interestingly, IgG titres against the three protein antigens studied, PspA, Ply, and PsaA were not found to significantly decrease in the elderly, suggesting immunological senescence in the form of decreased anti-protein antibody titres may not be a cause of increased susceptibility for IPD in the elderly [87]. Subsequent studies in the Philippines and Finland further supported the findings of the Kenyan study, demonstrating rapid kinetics in the development of IgG titres against pneumococcal protein antigens [88, 89]. Mothers in the Philippines were shown to have higher IgG titres on average compared to adults in Finland, though this is likely due to increased pneumococcal carriage rates amongst this population. Infants in this study were shown to develop IgG titres exceeding adult levels between 20 and 30 weeks of age against PsaA, while anti-Ply and anti-PspA IgG titres were not shown to reach adult levels over the 50-week study period [88]. A cohort study from Finland found that anti-PsaA IgG titres in infants exceeded adult titres by 6 months of age, while anti-Ply titres approached adult levels by 24 months of age. Anti-PspA titres were found to increase with slower kinetics, though this is likely due to high levels of PspA antigenic heterogeneity [89].

Further compelling evidence for the role of anti-protein antibodies in protection against pneumococcal carriage and disease arose from an experimental model of human carriage in adults. Healthy adult volunteers received an intranasal inoculum of pneumococcal serotype 23F. Susceptibility to carriage was more strongly linked to the absence of pre-existing antibody responses against a 22kDa protein – later identified as PspA – rather than pre-existing titres of IgG or IgA against the 23F capsule type [90]. Taken together, these studies demonstrate a key role for the anti-protein antibody response in protection against pneumococcal disease and carriage both early and later in life. As cross-reactivity between capsule serotypes is highly limited, the serotype-independent, age-related decline in pneumococcal disease is far more likely a result of the development of an immune response against highly conserved protein antigens, particularly in the early years of life. Considering this evidence, the anti-protein antibody response should be further investigated for the purpose of pneumococcal vaccination.

1.3. Treatment of pneumococcal disease

With the majority of pneumococcal disease cases occurring in developing countries, treatment of IPD and pneumococcal pneumonia generally relies on the oral administration of inexpensive antibiotics following diagnosis by primary healthcare workers. Amoxicillin and trimethoprim-sulphamethoxazole (TMP-SMX) remain frontline treatments for less severe cases in children, while more severe cases are often referred to hospital for administration of penicillin or chloramphenicol. Treatment options for adults include oral administration of tetracyclines in addition to antibiotics used in cases of childhood illness [91]. In developed countries, penicillin acts as a first line antibiotic against pneumococcal infection, with more severe cases treated in hospital through administration of broad-spectrum antibiotics until sensitivity testing has been undertaken [92].

Disturbingly, isolation of single- and multi- drug resistant strains of *S. pneumoniae* is becoming more frequent. Penicillin resistant strains have been isolated worldwide, with resistance occurring through the structural modification of pneumococcal penicillin-binding proteins, allowing the synthesis of peptidoglycan and new cell wall in the presence of the antibiotic [23, 93]. Resistance to TMP-SMX treatment is also highly prevalent worldwide, and often occurs

concurrently with penicillin- and macrolide- resistance [94, 95]. Increases in non-susceptibility to frontline treatments used in both developing and developed countries against pneumococcal disease has led to the development of prophylactic approaches, such as vaccination, in a bid to reduce the global burden of pneumococcal disease.

1.4. Pneumococcal vaccines

The generation of anti-capsular antibodies provides the current basis of pneumococcal vaccination. These antibodies are highly protective against IPD in a serotype-specific manner [96, 97], however, a number of shortcomings are limiting the impact of vaccination on the global burden of pneumococcal disease. This has led to continued interest in the development of novel pneumococcal vaccination strategies.

1.4.1. Purified polysaccharide vaccine (PPV)

The first widely available pneumococcal vaccine was released in the 1970s, and the current formulation contains purified polysaccharide antigen from 23 capsular serotypes (23vPPV). 23vPPV has been formulated to include polysaccharide from serotypes 1, 2, 3, 4, 5, 6B, 7F, 8, 9N, 9V, 10A, 11A, 12F, 14, 15B, 17F, 18C, 19F, 19A, 20, 22F, 23F, and 33F [98], and is currently recommended for use in Australia for healthy non-indigenous adults over 65 years old, healthy indigenous adults over 50 years old, and adults with an increased risk of IPD [99].

Despite boasting relatively high serotype coverage, 23vPPV is associated with significant shortcomings that have limited its effectiveness in reducing the global burden of pneumococcal disease. The key limitation of 23vPPV arises from the immunogenic nature of polysaccharide antigens, classified as T-independent (TI) immunogens. These antigens activate B cells primarily via natural killer (NK) cells with limited T-cell regulation in murine models [100]. In the absence of T cell help, polysaccharide antigens fail to induce memory responses, disproportionately favour IgM antibody production, and are poorly immunogenic in young children with the highest risk of IPD [101]. Furthermore, while 23vPPV is effective at preventing pneumococcal bacteraemia in the elderly, it is associated with limited efficacy in

preventing community-acquired, non-bacteraemic pneumonia in this cohort [102, 103]. Some studies also reported reduced serotype-specific immunogenicity of some 23vPPV antigens, particularly polysaccharide belonging to serotypes 3 and 4, with serotype 4 considered the leading cause of IPD in North America prior to the introduction of the protein-conjugate vaccine [104].

1.4.2. Protein Conjugate Vaccine (PCV)

A second class of pneumococcal vaccine, the protein conjugate vaccine (PCV), was first introduced in the early 2000s in an attempt to address some of the limitations associated with 23vPPV. This formulation contains polysaccharide antigen from a maximum of 13 serotypes (1, 3, 4, 5, 6A, 7F, 9V, 14, 18C, 19A, 19F, 23F) conjugated to a protein carrier, switching the antigen from a TI to T-dependent (TD) immunogen [105]. The switch from a TI to TD antigen restores immunogenicity in young children who failed to mount a protective response against polysaccharide-based 23vPPV, delivering protection to a key high-risk group for IPD. Furthermore, this switch also facilitates the development of a memory response and Ig isotype switching [81]. In Australia, 13vPCV is currently recommended for indigenous and non-indigenous infants and children younger than 5 years old, with indigenous children at a higher risk of IPD recommended to receive 4 doses rather than 3 [99].

PCVs have been demonstrated to be highly effective at preventing non-invasive and invasive pneumococcal disease caused by vaccine serotypes. Rates of AOM in young children have been reported to have decreased by 96% following the introduction of 7vPCV, and a further 85% following the introduction of 13vPCV [106]. The benefits of widespread use in young children have also extended to adult populations, with reduced childhood carriage rates leading to community-wide decreases in pneumococcal transmission in a serotype-specific manner. For example, rates of IPD in adults over 50 in the US have been reported to have decreased by up to 37% in the post-PCV era [107]. Despite enhanced immunogenicity in infants and the flow-on effects for the wider community, the high cost of manufacture limits antigen inclusion in PCV, limiting serotype coverage to 13. Furthermore, high costs can limit vaccine accessibility in developing countries where the burden of pneumococcal disease is highest [4].

1.4.3. Serotype replacement

While providing protection against vaccine-included serotypes, both 23vPPV and 13vPCV share a significant limitation in that they fail to offer protection against pneumococcal disease caused by non-vaccine serotypes (NVTs). Due to high levels of structural diversity in the polysaccharide chains of each capsular serotype, cross-reactivity of vaccine-induced immune responses is extremely limited. Not only does serotype specificity limit vaccine efficacy in different geographical regions, with coverage ranging from over 85% of circulating serotypes in the US, to 55% in Asia [13], but serotype specific vaccination is the driving force behind serotype replacement [108]. This occurs when the nasopharyngeal niche is vacated by serotypes targeted by vaccination and re-occupied by NVTs against which widespread pre-existing immunity is absent [3, 4, 13]. Subsequently, carriage and rates of disease caused by NVTs increases, reducing the impact of vaccination on the overall burden of pneumococcal disease.

Randomised placebo-controlled trials (RCTs), from the Gambia [109], South Africa [110], the Netherlands [111], and the US [112] have shown an increase in NVT carriage following vaccination with 7vPCV [108]. Rates of invasive disease caused by NVTs have also increased, with cohort studies from Wales identifying a 48% increase in NVT disease in adults older than 65, and a 68% increase in children under 2 [113]. Similarly, in the US, rates of NVT disease were found to increase from 44% before the introduction of PCVs (1998-1999) to 78% by 2004 [114]. Capsule-targeted vaccines also offer no protection against unencapsulated strains of *S. pneumoniae*, or non-typeable strains (NT-*Spn*). While the majority of clinical isolates of *S. pneumoniae* are encapsulated, with different serotypes showing varied propensities for causing disease [115], NT-*Spn*, are becoming more clinically relevant. NT-*Spn* has been associated with epidemic bacterial conjunctivitis [116], AOM [117], and invasive pneumococcal disease [118].

1.5. Experimental vaccines

Considering the limitations of current pneumococcal vaccines, a new approach is required to offer serotype-independent protection in all age groups in a cost-effective manner. Protein-based vaccines have become a focus of experimental pneumococcal vaccine research as, unlike the polysaccharide capsule, cell-surface proteins are highly conserved across serotypes. Furthermore, vaccinating against protein antigens may more closely mimic the natural development of the anti-pneumococcal immune response associated with age-related declines in pneumococcal disease.

1.5.1. Protein-based vaccines

Despite possessing an array of protein antigens, many studies focus on the protective effects of vaccinating with PspA, PsaA, and Ply. PspA represents an attractive vaccine antigen due to its exposure at the pneumococcal cell surface, protruding through the capsule to aid in interfering with complement fixation and lactoferrin binding [119, 120]. Vaccination of mice with full-length recombinant PspA has been shown to elicit protection in a serotype-independent manner in multiple studies [121, 122]. However, this serotype-independent protection is limited. While some cross-reactivity does exist, PspA is an antigenically variable molecule consisting of three major structural domains; the N-terminal domain, a proline-rich central domain, and a C-terminal domain. Major cross-reactive epitopes are predominantly located in the alpha-helical N-terminal domain, with antigenic variations allowing PspA molecules to be categorised into three distinct families, and six clades [123]. Thus, the serotype-independent protection offered by PspA may be restricted to serotypes within the same family as that used for vaccination. In contrast, the surface protein PsaA is highly conserved across pneumococcal serotypes [124]. Also exposed at the pneumococcal surface, PsaA acts as an ABC-type permease complex involved in the uptake of Mn^{2+} [125]. Vaccination of mice with antigenic PsaA peptides was shown to reduce carriage rates of serotypes 2, 4, and 6B [126]. Non-haemolytic pneumolysin toxoid has also been investigated as a vaccine antigen and has been demonstrated to offer protection in a serotype-dependent manner in mice. It has been hypothesised that differences in protection conferred against various serotypes depends on the role of pneumolysin in virulence of the challenge strain [127].

Despite offering some protection against pneumococcal disease and colonisation, single-antigen pneumococcal protein vaccines fail to elicit levels of protection comparable to those induced by vaccination with PCVs. Subsequently, the effect of combining protein antigens was investigated in an attempt to enhance immunogenicity of protein-based vaccines. Vaccination with multiple antigens was shown to have an additive effect on immunogenicity, with the combination of pneumolysin toxoid, PspA, and PspC providing the highest level of protection in mice compared to vaccination with each antigen alone, or in combination with other antigens [128].

1.5.2. Whole-cell inactivated vaccines

Whilst protein-based vaccines may appear to be an attractive alternative to PPVs and PCVs, the cost associated with large-scale protein expression and purification would likely become a limiting factor. High costs may limit both antigenic inclusion and restrict accessibility to vaccines in developing countries. Multiple groups have focused on an alternative approach to the protein-based vaccine using whole-cell, unencapsulated pneumococcal vaccine antigen.

Chemically inactivated pneumococcal vaccines

A number of chemical inactivation methods have been investigated in pursuit of generating a whole-cell, killed pneumococcal vaccine. Initially, ethanol treatment appeared to be the most effective option, generating a whole-cell antigen with enhanced immunogenicity when compared to antigens inactivated using more traditional methods such as heat [48], formalin, and UV radiation [129]. Administration of whole-cell, encapsulated pneumococcal antigens treated with ethanol was demonstrated to protect against intranasal carriage in mice and the development of pneumonia in rats following challenge with heterologous pneumococcal strains [130]. This robust immune response was reliant on intranasal administration of this vaccine with added cholera toxin adjuvant. While intranasal vaccination has the advantage of generating an immune response via the natural route of infection, the requirement for adjuvant to induce a strong immune response using this preparation prevents utilisation in humans until FDA-approved mucosal adjuvants become available [131].

In order to generate GMP-grade chemically inactivated pneumococcal vaccines, β -propiolactone (BPL) [132] and chloroform [133] have been utilised. While effective, these methods require further processing steps for the elimination of residual chemicals from the final vaccine preparation. Additionally, whole-cell vaccine preparations inactivated using ethanol, chloroform, trichloroethylene and BPL have been found to damage the microbial membrane, resulting in the solubilisation of approximately 15% of total protein content [129].

Gamma-irradiated pneumococcal vaccine

γ -irradiation is gaining more interest as a powerful vaccine inactivation method. Routinely, it has been used for the sterilisation of pharmaceutical products [134], food [135], and highly pathogenic materials, such as Ebola virus, for safe transportation [136]. γ -irradiation sterilises biological material through direct and indirect mechanisms. Direct damage occurs when gamma-rays cause the displacement of a molecule's outer shell electrons, leading to the ionisation of the molecule, and subsequent breakage of covalent bonds [137]. In microorganisms (and eukaryotic cells), this leads to the introduction of breakages into genetic material, preventing genome replication [138], whilst having a low overall effect on protein epitopes [139]. Most protein damage occurs via indirect damage when gamma-rays or ejected electrons interact with water molecules to generate oxidising free radicals [137]. Importantly, indirect damage can be minimised through optimisation of irradiation conditions to reduce the formation and movement of free radicals, whilst still permitting genome damage via direct mechanisms. This leaves protein antigens intact and immunogenic [140], whilst rendering the pathogen replication-incompetent and thus, killed. As a result, our γ -irradiated, whole-cell killed pneumococcal vaccine is completely killed and safe, and also highly immunogenic.

γ -irradiation has been proposed as a method to generate killed but metabolically active (KBMA)/non-dividing but metabolically active (NDMA) vaccines. As proteins both externally and internally are left intact, enzymatic activity is likely to be retained by irradiated, replication incompetent pathogens. This may allow for the unique pairing of the safety benefits of killed or subunit vaccines, with the enhanced immunogenicity of live-attenuated vaccines. This

enhanced immunogenicity is thought to be due to the immune system's ability to distinguish between live and dead pathogenic material. This distinction is essential for the fine-tuning of an immune response; too vigorous a response to non-infectious pathogenic material may lead to an inappropriate and damaging inflammatory response, while an insufficient response to a live pathogen may lead to the unchecked development of life-threatening disease [141]. Detection of vita-PAMPs (PAMPs associated exclusively with live pathogens) is thought to allow for pathogen viability assessment and appropriate scaling of the immune response [142, 143]. Prokaryotic RNA has been identified as a key vita-PAMP, with actively transcribed mRNA associated with enhanced inflammasome activation, IFN- β production and immunoglobulin class-switching [144].

A KBMA vaccine against *Listeria monocytogenes* was described in 2005 in which the genetically-modified microorganism was photochemically inactivated using psoralen and long-wavelength UV light. In addition to being replication incompetent, KBMA *L. monocytogenes* was shown to be capable of protein synthesis and induced a cellular immune response comparative in strength to that observed in mice vaccinated with the live bacterium. Contrastingly, no significant CD8+ T cell response was observed when mice were vaccinated with the heat-killed microorganism [145]. γ -irradiated *Brucella melitensis* has also been shown to be incapable of replication whilst maintaining metabolic activity as measured by Alamar Blue and luminescent promoter assays. Vaccination of mice with NDMA *B. melitensis* induced enhanced, long-term protective cytotoxic T lymphocyte (CTL) responses compared to vaccination with heat-killed *B. melitensis* [146]. The KBMA term has been modified to NDMA when applied to γ -irradiated *B. melitensis* due to the extent of DNA damage anticipated during each respective inactivation process. The KBMA method aims for minimal psoralen cross-linking events to maximise gene expression post-inactivation. Comparatively, γ -irradiation induces widespread genomic damage, reducing the availability of undamaged genes for expression [147]. Gene expression post-inactivation has never been compared between KBMA and NDMA organisms, however.

Our lab has been working on an alternative whole-cell pneumococcal vaccine. Rather than purifying a select panel of protein antigens, we have generated an unencapsulated derivative

of pneumococcal serotype 2, termed Rx1. Through the use of Rx1 as a whole-cell vaccine antigen, all pneumococcal proteins and other surface antigens are included in the vaccine preparation, effectively generating the highest valency pneumococcal vaccine to date. For safety purposes, the vaccine strain has been further attenuated through knock-out of the *lytA* (autolysin) and *psaA* genes, and replacement of the pneumolysin-encoding gene, *ply*, with non-haemolytic PdT. Whilst vaccination with purified PsaA has previously been demonstrated to induce serotype-independent protection in mice, removal of this highly immunogenic antigen for safety purposes does not reduce the overall immunogenicity of our vaccine preparation, with other protein antigens effectively compensating for the removal of this specific antigen. This highly attenuated strain (PN Δ PsaA) is then exposed to a sterilising dose of γ -irradiation, generating γ -PN Δ PsaA. As γ -PN Δ PsaA is unencapsulated, the immune responses generated against this pneumococcal vaccine are targeted against highly conserved protein antigens. Furthermore, as this vaccine is based on a whole-cell antigen, the costly process of protein expression and purification is avoided, potentially lowering manufacturing costs and increasing accessibility. Intranasal vaccination with a prior form of this novel vaccine (γ -PN) has been shown to induce serotype independent protection in mice following challenge with strains P9 (serotype 6A), EF3030 (serotype 19F), and D39 (serotype 2) in a B cell dependent manner [66].

1.6. Project rationale

This research investigated the enzymatic and metabolic activities of gamma-irradiated *Streptococcus pneumoniae* and mechanisms by which antibodies mediate protection against encapsulated pneumococci. The extent of enzymatic activities retained by irradiated pneumococci has not been described previously and is expected to provide novel insight into the generation of an NDMA-like vaccine. In addition, analysis of IgG functionality against encapsulated pneumococci could provide an insight into how antibodies function more broadly against encapsulated pathogens, aiding in the development of more effective vaccination strategies based on IgG subclass profiles.

The first part of this project investigated the possible retention of enzymatic activities by irradiated pneumococci. Gamma-irradiation has been proposed as an ideal method for the generation of whole-cell vaccines as antigenic proteins are left intact in their native conformation. As proteins remain relatively undamaged, I investigated if enzymes remained functional following killing of the whole-cell organism. This could be assessed in terms of the capacity for continued activity of pre-synthesised enzymes, and the retention of transcriptional and translational activities following killing. Importantly, gene expression by KBMA or NDMA organisms has not been demonstrated previously. In addition, a broad-spectrum indicator of metabolic activity could be used to assess whether or not irradiated pneumococcal antigens can be considered KBMA or NDMA for the purposes of vaccination.

The second part of this project investigated the vaccine-mediated antibody response against encapsulated strains of *Streptococcus pneumoniae*. As γ -PN Δ PsaA is formulated with an unencapsulated strain of *S. pneumoniae*, the immune response generated following vaccination is directed towards sub-capsular antigens, the majority of which are proteins. These antigens are highly conserved across pneumococcal serotypes, allowing for the generation of a protective, serotype-independent immune response. Whilst these sub-capsular antigens are readily accessible on the surface of unencapsulated pneumococcal strains, the majority of clinically relevant strains express varying levels of capsular polysaccharide implicated in the shielding of sub-capsular antigens from specific IgG. The vaccine-induced immune response has previously been shown to offer protection against challenge with encapsulated pneumococcal strains in a murine model, though the method by which vaccine-induced antibodies mediate protection against encapsulated pneumococci is yet to be elucidated. By manipulating capsule expression through growth under different conditions, this is expected to provide a novel insight into how protection against pneumococcal disease via antibody-mediated immunity occurs in terms of two key aspects. Firstly, as the pneumococcus is known to vary capsule expression *in vivo*, I addressed whether a specific pneumococcal phenotype is the target of vaccine-induced antibodies. Secondly, considering, specific IgG subclasses are associated with enhanced opsonophagocytic activity, I investigated the impact of changes in IgG subclass profiles on antibody binding to pneumococcal cells, aiming to elucidate an ideal subclass profile for opsonisation of encapsulated pathogens.

1.6.1. Hypotheses and aims

Hypotheses

1. Enzymatic activity is retained by *S. pneumoniae* receiving a sterilising dose of γ -irradiation
2. Total IgG binding to pneumococcal cells will be influenced by capsule expression
3. Different vaccination routes will be associated with changes in IgG subclass profiles in mice

Aims

Aim 1: Investigating the enzymatic and metabolic activity of γ -irradiated *S. pneumoniae*

- Aim 1.1: Investigate the retention of enzymatic activity by γ -irradiated pneumococci
- Aim 1.2: Analyse RNA expression from inducible genes by γ -irradiated pneumococci
- Aim 1.3: Examine metabolic activity by γ -irradiated pneumococci

Aim 2: Investigating the functionality of vaccine-induced antibodies against encapsulated strains of *S. pneumoniae*

- Aim 2.1: Analyse the cross-reactivity of γ -PN Δ PsaA immune sera against a wide range of pneumococcal serotypes
- Aim 2.2: Assess γ -PN Δ PsaA vaccine-induced IgG interactions with whole-cell encapsulated strains of *S. pneumoniae*
- Aim 2.3: Investigate the impact of vaccination route on IgG subclass profiles and total IgG binding

CHAPTER 2

Materials and Methods

2.1. Ethics statement

Animal work was conducted in strict accordance with the Australian Code of Care and Use of Animals for Scientific Purposes (7th edition 2004, 8th edition 2013) and the South Australian Animal Welfare Act 1985. Experimental protocols approved by AEC at the University of Adelaide. Ethics number: S-2016-183.

2.2. Growing bacterial stocks

To generate working stocks, 15-25µl of inoculum was taken from bacterial strain master stocks, streaked onto blood agar plates, and incubated at 37°C in 5% CO₂ overnight. Colonies were then collected from the plates and inoculated into pre-warmed growth media (serum broth, THY, SILAC + 0.5% glucose, galactose, or raffinose) to a start OD₆₀₀ of 0.05 – 0.07. Cultures were incubated at 37°C in 5% CO₂ and OD₆₀₀ checked periodically. When OD₆₀₀ reached 0.2, growth was stopped by placing the culture on ice. The culture was then distributed into 1ml aliquots for storage at -80°C or washed three times in PBS before resuspension in PBS + 13% glycerol for freezing in 1ml aliquots. Stocks were titrated by colony counts following serial dilutions (titres expressed as colony forming units (CFU)/ml).

Inactivation of the parent strain D39 and vaccine strain PNΔPsaA occurred via exposure of each preparation to 16 kGy of γ-irradiation from a Cobalt-60 (⁶⁰Co) source located at ANSTO, NSW. Samples were kept frozen on dry-ice during irradiation and transportation. Sterility of treated samples was confirmed by plating on blood agar plates.

2.3. Neuraminidase assay

Live and irradiated samples of D39 were plated in a 96-well flat-bottomed plate at $2.5 \cdot 10^5$ CFU/well in a volume of 25µl, with 0.125mM 4-MUNANA neuraminidase substrate. The plate was incubated at 37°C in 5% CO₂ for 2 hours before 100µl ice cold Na₂CO₃ stop solution was added to each reaction well. Fluorescence was read immediately (Ex = 365nm, Em = 450nm, automatic cut-off = 435nm) on a SpectraMax plate reader. The bacterial neuraminidase cleaves the 4-MUNANA substrate into fluorescent 4-MU, and NANA, thus the fluorescence

readout gives an indication of the retained functionality of pneumococcal enzymes after irradiation.

2.4. RNA extraction and qRT-PCR

γ -irradiated and live PN Δ PsaA were inoculated into SILAC (+ 0.5% raffinose, galactose, glucose, or no sugar) shock media from frozen stocks to a starting OD₆₀₀ of 0.25. Cultures were incubated at 37°C in 5% CO₂ for one hour before being placed on ice to stop transcription. OD₆₀₀ of each culture was measured and all were adjusted to match the lowest OD₆₀₀ reading. Pellets were generated from each culture by centrifugation of 2ml aliquots at 4°C, 13,000 rcf for 5 minutes. RNA was extracted from combined pellets by hot phenol extraction and collected following the Qiagen RNA extraction protocol. RNA concentration and purity were determined using a NanoDrop Microvolume Spectrometer and samples were stored in RNase free water at -80°C until use.

20 μ g/ μ l RNA samples were used as RNA template in PCR reactions. Each reaction mix consisted of 0.1 μ l Taq polymerase mixture, 5 μ l 2 \cdot SYBR green reaction mix, 0.2 μ l F and R primers (10 μ M), and 4 μ l DEPC-treated water per gene analysed (*rafK*, *rafG*, *galK*, *aga*). Gyrase A (*gyrA*) expression was used as an internal control for normalisation of RNA expression. 9 μ l of reaction mix was combined with 20ng of template RNA for plating on a 384 well tray. qRT-PCR was undertaken in a Light Cycler 480 II. See table 1 for primers.

Table 2.1. Primers used for qRT-PCR experiments

<i>rafK</i>	
F 5' AACGACGTAGCTCCAAAAGA 3'	R 5' GCTGGTTTACGTTCCAAGAA 3'
<i>rafG</i>	
F CCTATGGCAGCCTACTCCATC	R 5' GGGTCTGTGGAATCGCATAGG 3'
<i>galK</i>	
F 5' CACGTTTCTCTGGAGCATGA 3'	R 5' ATGGCACAGCCACTAAAACC 3'
<i>aga</i>	
F 5' AAGGTCAGAATGGTCCACAG 3'	R 5' GCTGGAAAATCAGCCATAAA 3'

<i>gyrA</i>	
F 5' ACTGGTATCGCGGTTGGGAT 3'	R 5' ACCTGATTTCCCCATGACAA 3'

2.5. Glucose utilisation assay

500µl of 0kGy or 16kGy irradiated D39 was thoroughly washed in PBS to remove glycerol (10,000 x g, 5 minutes). 500µl washed samples were inoculated into 10ml prewarmed SILAC media containing 1mM glucose. Cultures were incubated at 37°C in 5% CO₂ for 7 hours and OD₆₀₀ readings taken at the start and end of the incubation period to measure growth. At T₀ and T₇ endpoint, 1ml aliquots of each culture were taken and processed for glucose quantification assay. Bacteria were pelleted and supernatant collected before spinning through a 10kDa spin column to deproteinate (3,750rpm, 10 minutes, 4°C). Supernatant was stored at -80°C until use in glucose quantification assay. Glucose quantification was undertaken following the manufacturer's instructions contained in the Abcam Glucose Detection Kit (ab102517).

2.6. Generating serum

4 – 6-week-old female outbred Swiss mice were vaccinated three times intramuscularly (IM) with 50µl γ-PNΔPsaA +/- 10% alum or intraperitoneally (IP) with 100ul γ-PNΔPsaA, with doses delivered 2 weeks apart. Vaccines were normalised based on protein content with doses of 4.3mg/ml protein administered. Blood was collected by sub-mandibular bleeding following the second vaccination. After the final vaccination, mice were sacrificed by cervical dislocation and blood collected from the heart cavity. Collected blood was kept at room temperature for 45 minutes to allow for clotting before centrifugation at 13,000rpm for 5 minutes. Supernatant was collected and stored at -20°C.

2.7. Enzyme-linked immunosorbent assay (ELISA)

Antibody titres were determined by ELISA. COSTAR high affinity flat bottom ELISA plates were coated with 50µl 1 · 10⁸ CFU/ml Rx1 *lytA*^{-/-}PdT and incubated at 4°C overnight. Wells were washed three times with PBS + 0.5% Tween20, and the remaining protein binding sites were blocked with PBS + 2% (w/v) skim milk blocking buffer at room temperature for 2 hours. Serum was serially diluted 1:2 in PBS by 1:2 from a starting dilution of 1:40, and added to the

appropriate washed wells, and the plate incubated for 2 hours at room temperature. Following washing, 50µl of goat anti-mouse IgG (H+L)-HRP (31430, ThermoFisher Scientific) was added to each well at a dilution of 1:10,000. After incubation for 2 hours at room temperature, wells were washed and 75µl of TMB colour developer solution was added. The plate was incubated in the dark for 20-30 minutes before the reaction was stopped by the addition of 50µl sulphuric acid. Absorbance of each well was read immediately at 450/620nm on a SpectraMax plate reader.

2.8. Flow cytometry

100µl of $1 \cdot 10^8$ CFU/ml *S. pneumoniae* (Rx1, D39 (serotype 2), serotype 3) was plated in a 96-well U-bottomed plate, topped up to 200µl with filter sterilised (f.s) PBS and centrifuged at 3,750rpm, 10 minutes, 4°C to pellet. Pellets were resuspended in 50µl diluted murine primary antibody (γ-PNΔPsaA immune sera from mice vaccinated IM + alum or IP) f.s PBS + 1% w/v BSA. Plates were incubated on ice for 45 minutes, then washed three times by centrifugation and resuspension in f.s PBS as described above. Following the final wash, pellets were resuspended in 50µl of AlexaFluor 488 conjugated goat anti-mouse IgG (H+L) at 1:2,000 in f.s PBS + 1% w/v BSA and incubated in the dark on ice for 45 minutes. Plate was washed three times with f.s PBS, and pellets were resuspended in 200µl f.s PBS + 2% (v/v) PFA. Events were acquired on an Accuri flow cytometer and analysed with FlowJo software. A minimum of 10,000 events were acquired per sample.

2.9. LRR fixation and capsule transmission electron microscopy (TEM)

Lysine ruthenium red fixation (LRR fixation) was used for visualisation of capsular polysaccharide by TEM with guidance from Dr Lisa O'Donovan and Ms Ruth Williams at Adelaide Microscopy. Fresh cultures of pneumococci (D39 (serotype 2) or serotype 3) were grown for fixation following the growth methods detailed previously, however, all cultures were centrifuged and washed gently to prevent loss of capsular material (slow acceleration/deceleration, gentle resuspension of pellets). Washed pellets were gently resuspended in formaldehyde/glutaraldehyde fixative (provided by Adelaide Microscopy) containing 0.075% (w/v) ruthenium red and 0.075M lysine acetate (LRR fixative) and

incubated on ice for 20 minutes. LRR fixative was removed and replaced with fixative containing 0.075% ruthenium red only (RR fixative) and incubated at 4°C overnight. Further fixation steps were undertaken at Adelaide Microscopy following their preestablished protocol. Briefly, samples were washed twice in PBS + 4% sucrose with 0.075% RR (RR wash) at room temperature. Pellets were fixed in PBS + 2% osmium and 0.075% RR for 1 hour before two RR washes. Pellets were dehydrated sequentially in 70%, 90%, and 100% ethanol (3 changes, 10-minute incubations) followed by a 15-minute incubation in 100% propylene oxide. Pellets were then incubated in a 1:1 mix of propylene oxide and resin for 1 hour, before being incubated overnight in 100% resin. Resin was changed three times the following day and polymerised at 70°C for a minimum of 24 hours following the final resin change. Samples were rotated during all incubation steps until polymerisation. Images were taken using an FEI Technai G2 Spirit TEM. Capsule measurements were made using ImageJ software.

2.10. Uronic acid capsule quantification

Fresh pneumococcal cultures (D39 (serotype 2) or serotype 3) were grown following the growth methods detailed previously, however, cultures were pelleted once and resuspended in 500µl reaction buffer (150mM Tris, 1mM MgSO₄, pH 7.0 in MilliQ water). 5µl 10% DOC was added, and suspension incubated at 37°C for 30 minutes to lyse cells. 10µl mutanolysin (100U), 5µl DNase, and 5µl RNase was added, and suspension incubated at 37°C in 5% CO₂ overnight. 5µl proteinase K was added, and suspension incubated at 54°C for 4 hours. Suspensions were briefly centrifuged to pellet debris and stored at -20°C until use.

Capsule suspension was serially diluted ½ four times in MilliQ water in duplicate. 100µl of diluted samples was added to 600µl H₂SO₄/Na₂B₄O₄ (sulphuric acid/sodium tetraborate solution, 0.0125M Na₂B₄O₄ in concentrated H₂SO₄) in 2ml safe lock Eppendorf tubes on ice in duplicate for each dilution. Tubes were briefly vortexed and incubated at 95°C for 5 minutes. Tubes were cooled on ice before addition of 3-phenylphenol solution or 0.5% NaOH. 10µl 3-phenylphenol (0.15% (w/v) 3-phenylphenol in 0.5% NaOH) or 0.5% NaOH was added to each tubes of each dilution (3-phenylphenol to one tube, 0.5% NaOH to duplicate tube/dilution).

Tubes were shaken immediately to mix and 200µl transferred to wells of a 96 well flat-bottomed tray. Absorbance was measured within 5 minutes of plating at 520nm.

2.11. Western blotting

1ml aliquots of various *S. pneumoniae* strains (serotypes 4, 19F, 3, 1, 19A, 6A, 10, 15B, 11A, 22, 29, 2, strain Rx1) at approx. $1 \cdot 10^8$ CFU/ml) were lysed by sonication in a Bioruptor for 30 cycles (30sec on/30sec off) with 0.04g acid-washed glass beads (Sigma, G4649). Protein content of lysed cultures was measured using the Pierce BCA protein assay kit (Thermo Scientific, cat no. 23225) as per the manufacturer's instructions. Aliquots of each lysate were made to a final protein concentration of 800µg/ml and 1· LUG buffer was added. Samples were boiled at 95°C for 5 minutes, and 25µl was loaded per well on a 12 or 17-well NuPage 12% Bis-Tris protein gel (Invitrogen, cat no. NP0349BOX) in a western tank filled with 1· MES running buffer. Gels were run for 22 minutes, 200V, mA: 500.

Separated proteins were then transferred to nitrocellulose membranes using a ThermoFisher iBlot transfer system and NOVEX mini kit. The membrane was then blocked in 20ml PBS + 5% (w/v) skim milk blocking buffer for 2 hours on a shaker table. Immune serum from γ-PNΔPsaA-vaccinated mice (IM +/- alum) was added directly to the blocking buffer at dilutions of 1:5,000, 1:10,000, or 1:25,000 and the membrane was incubated at room temperature overnight with shaking. The membrane was washed three times in PBS + 0.5% tween before ODYSSEY IRDye goat anti-mouse 800 secondary antibody was added at a dilution of 1:50,000 in 20ml PBS + 0.5% tween + 0.05% w/v skim milk. The membrane was incubated in the dark at room temperature for 2 hours on the shaker table. Following three washes, excess liquid was removed from the membrane, followed by incubation at 37°C for 15 minutes. The dry membrane was then visualised using a LI-COR ODYSSEY machine and software.

2.12. Coomassie staining

25µl of 800µg/ml whole cell lysates (generated as above) were run on 17-well NuPage 12% Bis-Tris protein gels. Gels were covered with Coomassie stain and boiled for 2 minutes followed by incubation for 10 minutes with shaking at room temperature. The coomassie stain

was removed and the gel rinsed with water until the water ran clear. The gel was then covered with destain solution and boiled for 2 minutes followed by a minimum of 30 minutes incubation at room temperature with shaking. Destain was removed and replaced with water prior to imaging of the gel with a GelDoc camera.

2.13. Statistical analysis

GraphPad Prism v. 7.0c for Mac was used for statistical analysis, with quantitative results expressed as mean +/- SEM. Statistical significance was determined by one or two-way ANOVA, or unpaired t-test, with P values <0.05 considered statistically significant (* $P <0.05$, ** $P <0.01$, *** $P <0.001$, **** $P <0.0001$).

CHAPTER 3

Results

3.1. The enzymatic activity of gamma-irradiated *S. pneumoniae*

Gamma-irradiation has been investigated as an inactivation method for a number of experimental vaccines against challenging pathogens and illnesses. Varying degrees of success have been observed in animal and human models when applying gamma-irradiation technology to pathogens such as *Schistosoma mansoni* [148], Venezuelan Equine Encephalitis Virus (VEEV) [149], and malaria [150] for vaccine development. In humans, gamma-irradiated vaccines have been examined in Phase 1 clinical trials against metastatic melanoma [151], and more recently, HIV-1 [152]. In addition to *Streptococcus pneumoniae*, members of our lab have used gamma-irradiation to inactivate influenza A virus, generating a whole-virus vaccine capable of inducing cross-reactive T cell responses in mice [153], and have examined the application of this technology to the generation of a rotavirus vaccine [154].

Exposure to low doses of gamma-irradiation is expected to primarily affect genetic material, with limited impact on protein antigens and their native conformation. While previous studies from our lab illustrated the immunogenicity of γ -PN, these studies did not investigate the enzymatic or metabolic activity of gamma-irradiated *S. pneumoniae*. Interestingly, other groups have classified gamma-irradiated *L. monocytogenes* [145] and *B. melitensis* [146] as KBMA or NDMA primarily on the basis of the retained ability to synthesis new proteins. In this study, I aimed to provide a more thorough investigation into multiple pathways that may remain viable and functional in a KBMA/NDMA-like organism after treatment with gamma-irradiation. Firstly, I assessed the retention of enzymatic activity, with focus on a key enzyme involved in pneumococcal virulence, neuraminidase. Secondly, the activity of transcriptional machinery was assessed through the measurement of new mRNA produced from inducible genes. Finally, I examined whether the maintenance of these pathways culminated in the

retention of metabolic activity in a broader sense, via assaying glucose uptake as an indicator of metabolic activity.

3.1.1. Retention of enzymatic activity by inactivated pneumococci

The neuraminidase activity of *S. pneumoniae* was used as read out to assess the enzymatic activity of pneumococci killed using gamma-irradiation, heat, or ethanol treatment (**Fig. 3.1.**). Samples of D39 (serotype 2) were either left un-irradiated (0 kGy live control), or killed by exposure to 16kGy of gamma-irradiation on dry-ice. Rx1, the vaccine strain, was not utilised as this strain does not possess measurable neuraminidase activity. It is hypothesised that retention of secreted neuraminidase enzymes is reliant on the presence of the pneumococcal capsule, and thus used the encapsulated parental strain, D39, for this experiment. My data show that while irradiated pneumococci lost a significant amount of neuraminidase activity compared to the non-irradiated (0kGy) control, the reduction in activity was significantly less severe than that observed for heat-inactivated or ethanol-killed samples. In fact, heat-killed pneumococci did not exhibit any neuraminidase activity, with RFU equivalent to background fluorescence observed in the PBS control group. Interestingly, ethanol-killed pneumococci retained low levels of neuraminidase activity. In addition, unexpectedly I did not detect any neuraminidase activity for Rx1, which is unencapsulated derivative of D39. Considering that neuraminidase is a secreted enzyme, the capsule may therefore be required for the retention of this enzyme throughout the washing steps utilised to generate bacterial cultures. Repetition of this experiment using media taken directly from an Rx1 culture may help investigating the lack of neuraminidase activity in our experimental settings.

3.1.2. RNA expression by irradiated pneumococci

In order to examine the capacity of gamma-irradiated pneumococci for gene expression at the transcriptional level, I analysed gene expression from four sugar-controlled inducible genes using qRT-PCR (**Fig 3.2.**). Specifically, I analysed genes induced by the sugar raffinose, including *aga* (**Fig. 3.2.A**), *rafK* (**Fig 3.2.C**), and *rafG* (**Fig. 3.2.D**). The expression of a galactose-controlled gene, *galK* (**Fig. 3.2.B**), was also examined. These genes were selected as the vaccine strain is known to possess them, and to respond at a transcriptional level to the presence of their respective inducing sugars. RNA was extracted from live PN(Δ PsaA) cells

grown in different conditions including SILAC media without sugar (no sugar) , SILAC supplemented with glucose, and SILAC supplemented with the inducing sugar for each gene. Importantly, the no sugar and glucose groups acted as controls for gene expression of *aga*, *rafK*, *rafG*, and *galK* under non-inducing conditions. Strong induction of these genes was detected in the appropriate conditions for the live 0 kGy PN(Δ PsaA) samples. Surprisingly, I also detected production of mRNA in response to these sugar-based stimuli for irradiated pneumococci samples. While 16kGy irradiated bacteria trended towards producing fewer transcripts from the *aga* and *galK* genes, there was no statistically significant difference in expression rates when compared to the 0kGy control under inducing conditions. Conversely, 16kGy irradiated bacteria produced significantly fewer transcripts from the *rafK* and *rafG* genes compared to their live counterparts under inducing conditions. Regardless, 16 kGy irradiated pneumococci produced detectable transcripts for all four genes compared to control no sugar and glucose samples. Expression levels in all experiments were normalised to *gyrA* expression.

3.1.3. Glucose utilisation as an indicator of broad-spectrum metabolic activity

Considering the retention of enzymatic and transcriptional activities, I investigated the possibility that irradiated bacteria may be capable of utilising glucose as a carbon source for metabolic activities (**Fig. 3.3**). Non-irradiated (0kGy) live bacteria (D39) were inoculated into SILAC supplemented with 1mM glucose growth media to a starting OD₆₀₀ of 0.04, while 16 kGy irradiated bacteria was inoculated to either the same starting OD₆₀₀ of 0.04 (low), or to a higher starting OD₆₀₀ of 0.1 (high). This high starting titre was intended to replicate the final bacterial burden of the live control at the end of the assay, given that the irradiated pneumococci cannot replicate. Quantification of glucose at the end of the 7-hour growth period showed a significant amount of glucose was consumed over the course of the assay by live (0 kGy) pneumococci. Conversely, the 16kGy irradiated bacteria inoculated at either a low or high starting OD₆₀₀ failed to consume a measurable amount of glucose. Given that sugars in culture media are readily imported for utilisation by irradiated pneumococci as illustrated in Fig. 3.2, this lack of glucose consumption is unlikely to be a result of a failure in sugar sensing or internalisation.

3.2. Humoral responses induced by γ -PN(Δ PsaA) and their interactions with encapsulated strains of *S. pneumoniae*

Previous publications illustrated that vaccination with γ -PN induces B-cell mediated, serotype-independent protection against lethal pneumococcal challenge in a murine model [66]. As gamma-irradiation allows for the preservation of proteins in their native conformation, antibody responses induced by γ -PN(Δ PsaA) are expected to target commonly shared surface pneumococcal protein antigens. In addition, considering the encapsulated nature of wild-type *S. pneumoniae* serotypes and the possible effect of the polysaccharide capsule on shielding protein antigens, it is important to investigate the effect of capsule expression on interactions between γ -PN(Δ PsaA) induced antibodies and sub-capsular protein antigens. In fact, the exact mechanism by which protein-specific antibodies can bypass the outer capsule layer of wild-type pneumococci is currently unknown. Thus, the highly reactive antibodies against a suite of sub-capsular protein antigens induced following vaccination with γ -PN(Δ PsaA) could be used to investigate how these antibodies interact with encapsulated pneumococci. Of note, the pneumococcus is known to vary capsule expression under different environmental conditions, which may mean that certain phenotypes are more readily targeted by vaccine-induced protein-specific antibodies. For example, capsule expression is downregulated during colonisation, exposing sub-capsular adhesins to the host environment to mediate adherence [60]. Conversely, enhanced capsule expression is required for the progression to an invasive phenotype, with the capsule conferring essential resistance to opsonophagocytic clearance in the blood [4]. Thus, exposing pneumococci to different growth conditions could be utilised to manipulate capsule expression to gauge which capsular phenotype may be more susceptible to binding by γ -PN(Δ PsaA)-induced protein-specific antibodies. Furthermore, I investigated the impact on antibody subclass profiles on total antibody binding to encapsulated pneumococci, to determine if a specific subclass was best suited to opsonising encapsulated pathogens.

3.2.1. Cross-reactivity of γ -PN(Δ PsaA)-induced antibodies against different pneumococcal serotypes

Previous studies have demonstrated *in vivo* protection against heterologous serotypes 6A and 19F, and homologous serotype 2 [66]. Given that the formulation of γ -PN(Δ PsaA) was based on an unencapsulated derivative of serotype 2, the observed protection was considered serotype-independent. However, the broad cross-reactivity of vaccine-induced immunity against a wider range of pneumococcal serotypes had not been assessed. For this, I examined the breadth of γ -PN(Δ PsaA)-induced antibody cross-reactivity against whole-cell lysates of PCV included and non-included pneumococcal serotypes using Western Blot. As shown in **Fig. 3.4.A** serum from γ -PN(Δ PsaA) vaccinated animals were able to react to every single pneumococcal serotype tested, demonstrating the broadly-reactive serotype-independent immune responses induced by this gamma-irradiated pneumococcal vaccine. Importantly, the whole-cell lysates tested in this experiment were prepared from live non-irradiated pneumococci, and the high intensity banding patterns indicate high specificity of vaccine-induced antibodies for these native protein antigens. Reactivity banding patterns were also highly consistent against proteins expressed by the range of PCV-included and non-included serotypes tested in this assay, with reactivity against serotype 3 lysate being the only notable exception as banding intensity was lower against some proteins despite the similar banding pattern. Coomassie staining of each lysate showed equivalent protein content in each lane (**Fig. 3.4.B**).

3.2.2. The effect of growth medium on capsule expression

To assess the binding of vaccine-induced antibodies to whole encapsulated pneumococci, I attempted to generate a panel of bacteria expressing different levels of capsular polysaccharide through growth in different mediums. Transmission electron microscopy (TEM) was used to assess which growth mediums would impact capsule expression and thickness most dramatically. The representative TEM images presented in **Fig. 3.5.A** show D39 (serotype 2) grown in serum broth to have a surface densely packed with short capsular polysaccharide chains. Comparatively, THY-grown D39 appeared to have polysaccharide chains of approximately the same length as chains on serum broth grown D39, but these chains appeared to be more sparsely packed (**Fig. 3.5.B**). Interestingly, SILAC + 0.5% glucose-grown D39 appeared to express the longest polysaccharide chains relative to the cell wall thickness (**Fig. 3.5.C**).

Quantitative analysis of capsule thickness (**Fig. 3.6.A**) and total capsular polysaccharide production using uronic acid capsule quantification (**Fig. 3.6.B**) provided further insight into the influence of growth media on capsule production and structure. This analysis indicated that serum broth- and THY-grown D39 expressed capsules of a similar thickness, both measured to be approximately 60nm thick. Comparatively, SILAC + 0.5% glucose-grown bacteria expressed a significantly thicker capsule with an average thickness of approximately 130nm. Despite expressing capsules of similar thicknesses, serum broth- and THY grown-D39 produced different amounts of total capsular polysaccharide. Serum broth grown-D39 produced approximately 40% less polysaccharide compared to THY grown-D39. This provided further insight into the capsule structure revealed by TEM imaging. While appearing similar structurally in terms of polysaccharide chain length, these chains must be more sparsely distributed over the surface of serum broth-grown cells compared to their THY-grown counterparts. Surprisingly, SILAC + 0.5% glucose and THY grown-D39 expressed similar levels of total capsular polysaccharide. While SILAC + 0.5% grown bacteria trended towards producing slightly less capsule than THY grown-D39, this trend was not significant. The combination of TEM imaging data and uronic acid capsule quantification suggests that changes in growth conditions have an impact not only on polysaccharide chain length, but also the amount of polysaccharide expressed on the surface of the pneumococcal cell.

The impact of these same growth conditions on capsule expression were similarly determined for serotype 3. TEM images showed serotype 3 cells grown in serum broth exhibited a dense capsule, however, the polysaccharide chains appeared to be much longer than those on the D39 counterpart (**Fig. 3.7.A**). Growth in THY resulted in the generation of a “patchy” capsule, with regions of densely packed, long and short polysaccharide chains (**Fig. 3.7.B**). Interestingly, growth in SILAC + 0.5% glucose resulted in highly variable capsule expression. While some cells appeared to express thick capsules like their D39 counterparts, others expressed a comparatively thin capsule. This was observed for multiple SILAC-grown pneumococci cells visualised in this manner, with images presented in **Fig. 3.7. C and D** being representative of the two ‘phenotypes’ observed.

Unlike D39 grown in serum broth and THY, serotype 3 grown in these mediums expressed capsules of significantly different thicknesses, with serum broth grown cells expressing a capsule with an average diameter of 300nm, compared with an average thickness of less than 100nm when grown in THY. Serotype 3 cells were selected as they produce thick capsules, thus allowing differences in capsule structure to be observed more easily. No significant difference in capsule thickness was observed when comparing serum broth or THY grown cells to SILAC + 0.5% glucose due to high levels of variability in this population. SILAC + 0.5% glucose grown cells, however, on average, exhibited thicker capsules than their THY grown counterparts (**Fig. 3.8.A.**). Interestingly, despite significant variability in capsule thickness between groups, no significant difference in total CPS content between all three groups was observed by uronic acid capsule quantification (**Fig. 3.8.B.**).

3.2.3. Antibody binding to encapsulated serotype 2 (strain D39)

While Western Blot analysis demonstrated high levels of cross-reactivity for vaccine-induced antibody responses against pneumococcal proteins, recognition of these antigens *in vivo* is complicated by the variable expression of the polysaccharide capsule in different anatomical niches. To address the possible effect of capsule expression on antibody interactions, I used pneumococci grown in various mediums to mimic variation in capsule expression and tested antibody binding using flow cytometry analysis. In this assay, cells were incubated with primary immune sera from vaccinated animals and stained with FITC-conjugated secondary antibody against murine IgG prior to flow cytometry analysis. As a control, pneumococci were treated with secondary antibody alone. Serotype 2 (D39) pneumococci grown in serum broth, THY, or SILAC media were probed with primary immune sera from mice vaccinated via the IP route with three doses of γ -PN(Δ PsaA) (**Fig. 3.9**), or mice vaccinated via the IM route with three doses of γ -PN(Δ PsaA) + alum adjuvant (**Fig. 3.10**). IP vaccination was utilised to generate very high titre 'hyper immune' sera, whilst IM + alum vaccination was used to mimic the administration route that will be adopted for clinical application of the whole inactivated vaccine. When using serum from IP immunised mice, IgG binding against D39 grown in serum broth demonstrated extremely low levels of antibody reactivity, with no significant difference in geometric mean fluorescence intensity (GMFI) observed between bacterial cells treated with primary antibody versus cells treated with secondary antibody only as a control. THY grown

cells demonstrated a significant increase in GMFI relative to their secondary antibody only counterpart, however, total IgG binding remained relatively low. Interestingly, IgG binding was highest when SILAC + 0.5% glucose grown cells were used, with a very clear positive shift in FITC fluorescence. A GMFI of approximately 7000 was observed, compared with < 1000 for serum broth or THY grown cells.

Interestingly, when probing the same D39 bacterial samples with serum generated by IM vaccination with γ -PN(Δ PsaA), these trends were completely reversed (**Fig 3.10**). Here, I observed IgG binding was highest using cells grown in serum broth, followed by THY, and SILAC + 0.5% glucose grown cells. Statistically significant increases in GMFI were achieved when treating cells grown in serum broth or THY only, whilst SILAC + 0.5% glucose grown cells showed a slight change in GMFI, without reaching statistical significance. Additionally, the background level of FITC fluorescence detected for serum-broth grown D39 was very high, suggesting some level of non-specific adsorption of the secondary antibody alone to the serotype 2 capsule. Regardless, the level of fluorescence detected when cells were stained with both primary and secondary antibodies was vastly higher, indicating the majority of signal detected was mediated by protein-specific vaccine induced antibodies.

3.2.4. The effect of vaccination route on IgG subclass profiles

Given the large variability between reactivity of immune sera generated using IP versus IM vaccination to encapsulated pneumococci by flow cytometry, I next assessed whether the IgG subclass profiles differed between the two types of immune sera. Direct ELISAs were conducted to measure the relative amount of IgG subclasses IgG1, IgG2a, IgG2b and IgG3 in the murine serum samples. As shown by **Figure 3.11.A**, vaccination by the IP route generated an IgG subclass profile that is not dominated by any single IgG subclass. Relative titres of IgG1 were not significantly different compared with titres of the remaining IgG subclasses. However, I detected a clear hierarchy between IgG2a, IgG2b and IgG3. Relative titres of IgG3 were significantly higher than IgG2b, with both IgG2b and IgG3 being significantly higher than IgG2a. Data related to sera generated using the IM route of vaccination with γ -PN(Δ PsaA) without alum showed an even distribution of the four IgG subclasses, although relative titres of IgG1 were highest (**Fig. 3.11.B**). In contrast, immune sera from mice vaccinated with γ -

PN(Δ PsaA) + alum showed a very clear shift in the IgG profile as antibody responses were largely dominated by the IgG1 subclass, followed by IgG2b with minimal levels detected for IgG2a and IgG3 (**Fig. 3.11.C**).

3.2.5. Antibody binding to encapsulated serotype 3

To further investigate whether there exists an ‘optimal’ subclass profile for binding to encapsulated pneumococci, binding experiments to encapsulated pneumococci were repeated using serotype 3. This serotype is renowned for expressing some of the highest levels of capsule of all pneumococcal serotypes, and thus was selected as a model to best identify Ig subclasses most suited to penetrating the capsule layer. Similarly, serotype 3 pneumococcal cells were grown in serum broth, THY, or SILAC + 0.5% glucose medium, and binding of pneumococcal-specific antibodies was assessed by flow cytometry following treatment of cells with serum from IP vaccinated mice (**Fig. 3.12**) or IM + alum vaccinated mice (**Fig 3.13**). An IM without alum group was not included due to lack of statistical significance among the levels of IgG subclasses shown in Fig. 3.11.B.

Interestingly, probing serotype 3 pneumococcal cells with serum from IP vaccinated mice generated an IgG binding trend different to that seen against D39 grown under the same conditions. While immune sera from IP vaccinated mice could not bind at all to serum broth-grown serotype 2 (**Fig. 3.9**), this immune sera bound significantly better to serum broth-grown serotype 3 when compared to the binding profile of the secondary antibody only control. This immune sera also effectively bound to THY-grown and SILAC-grown serotype 3, with significant increases in FITC signal above the background fluorescence levels for each culture type. Of the three, SILAC + 0.5% glucose cultures showed the highest overall GMFI for IgG binding, which is similar to what was observed for IgG binding to serotype 2, though this difference was far less obvious for serotype 3.

Additionally, all three cultures of serotype 3 showed statistically significant increases in GMFI relative to their secondary antibody only controls when probed with sera from mice vaccinated via the IM route with γ -PN(Δ PsaA) + alum (**Fig. 3.13**). IgG binding was approximately equivalent between serum broth and SILAC + 0.5% glucose-grown cells, while binding to

THY grown-cells was substantially lower. Regardless, this immune sera was able to significantly bind to all three culture types. This trend actually mimics what was seen when probing the same serotype 3 cultures with sera from mice vaccinated via the IP route indicating that serotype 3 shows similar increases in FITC signal regardless of the vaccination route.

Taken together, these data reveal a complex interplay between IgG subclass profiles, capsule characteristics, and pneumococcal serotypes. The role of the capsule in sub-capsular antigen shielding, however, remains clear, with increases in GMFI consistently lower when using serotype 3 cells versus serotype 2 cells with thinner capsules. Despite this, while no clearly beneficial subclass profile emerged, an encouraging observation was found in that IgG appears to be capable of binding protein antigens expressed by pneumococci concurrently expressing a thick polysaccharide capsule. Whether this comparatively lower level of IgG binding translates to preserved OPKA, however, is yet to be determined.

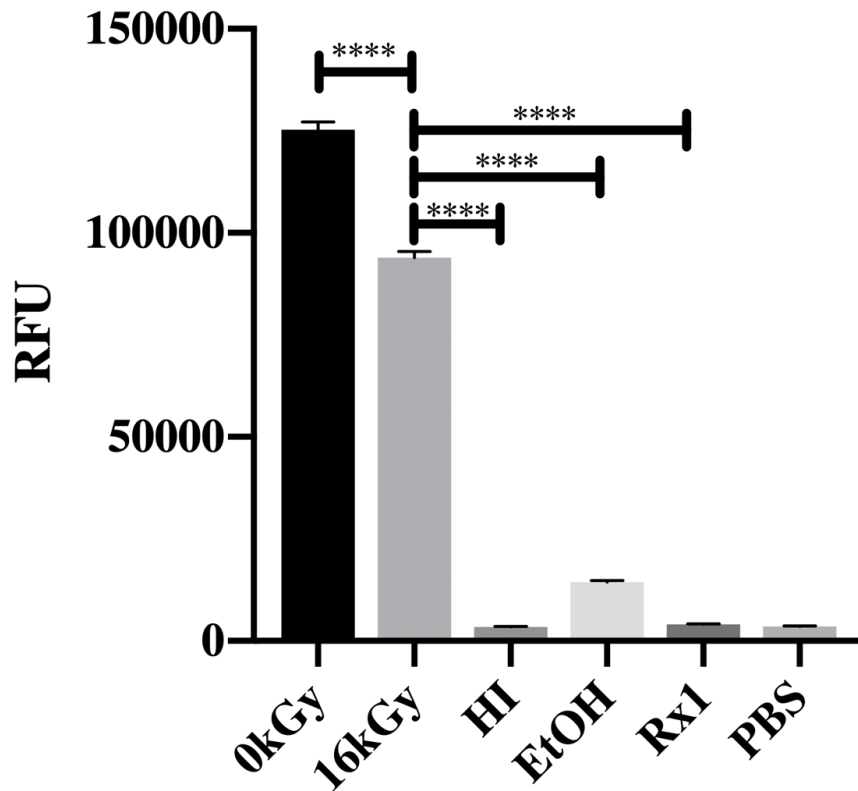


Figure 3.1. Neuraminidase activity of strain D39 (serotype 2) and Rx1 pneumococci inactivated using different mechanisms. Live pneumococci (0kGy), pneumococci inactivated using gamma-irradiation (16kGy), heat (HI), or ethanol (EtOH), and an unencapsulated derivative (Rx1) were incubated in PBS for two hours with a non-fluorescent neuraminidase substrate, 4-MUNANA. Cleavage of this substrate by active neuraminidase produces a fluorescent product, 4-MU, and this activity was measured in terms of relative fluorescence units (RFU). Statistical significance analysed by one-way ANOVA (* $P < 0.05$, ** $P < 0.01$, *** $P < 0.001$, **** $P < 0.0001$, n.s. = not significant). Data presented as mean \pm SEM (n = 3). Data indicative of a single experiment.

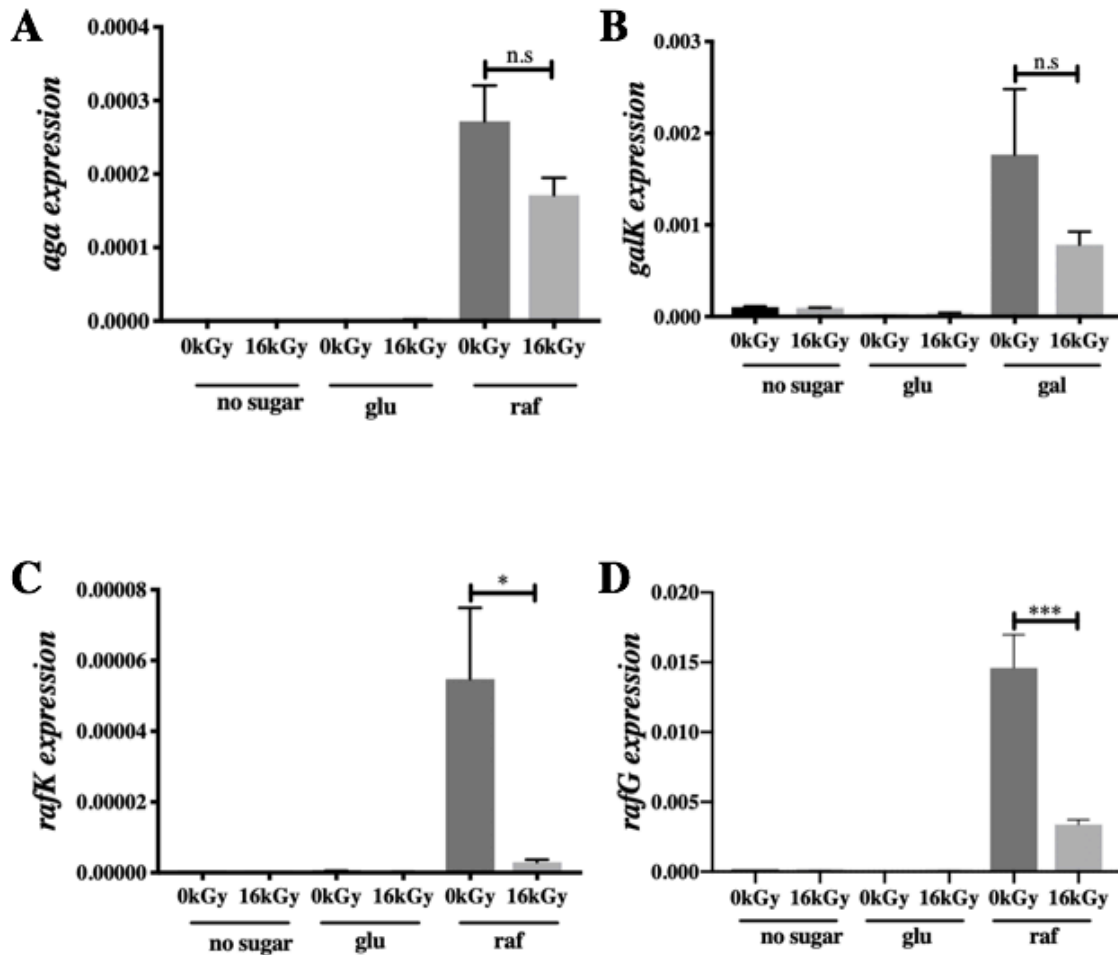


Figure 3.2. qRT-PCR of inducible genes controlled by the raffinose and galactose operons under inducing and non-inducing conditions. Live (0kGy) and irradiated (16kGy) PN Δ PsaA were incubated under growth permissive conditions in which no sugar, glucose, or an inducing sugar (raffinose or galactose) was available as the primary carbon source. After one hour, RNA was harvested using hot phenol extraction and purified. Expression of *aga* (A), *galK* (B), *rafK* (C), and *rafG* (D) were normalised to *gyrA* expression. Statistical significance analysed using unpaired t-test (* $P < 0.05$, ** $P < 0.01$, *** $P < 0.001$, **** $P < 0.0001$, n.s. = not significant), data presented as mean \pm SEM (n = 2) and indicative of a single experiment.

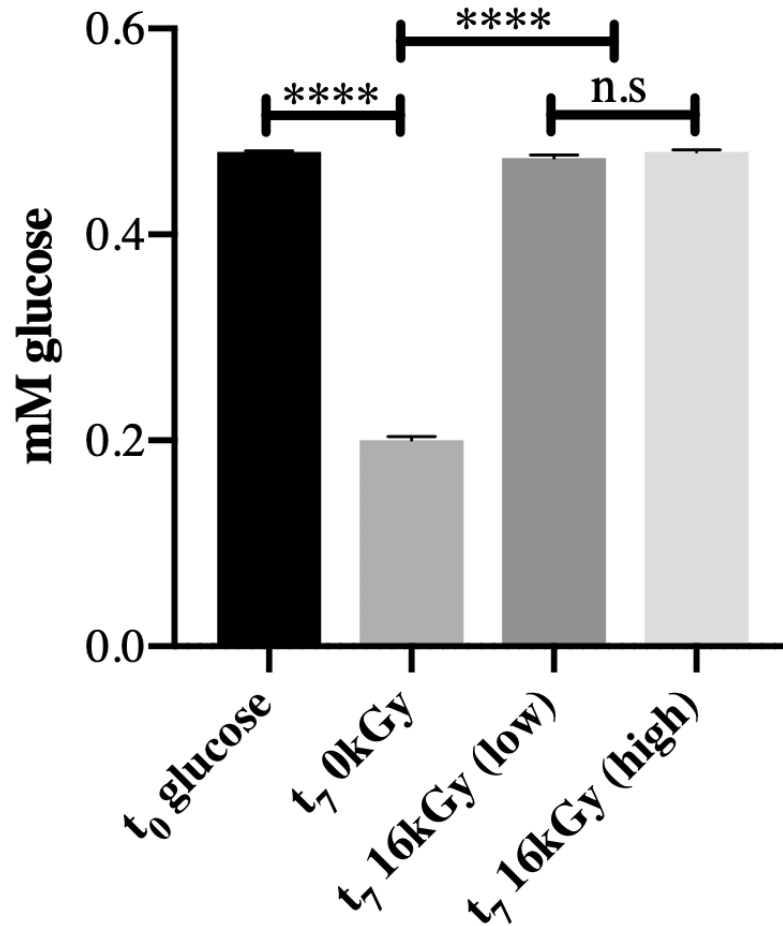


Figure 3.3. Glucose utilisation by live (0kGy) and irradiated (16kGy) Rx1 pneumococci. Bacteria were incubated under growth permissive conditions in SILAC + 1mM glucose. Starting glucose content was measured at t_0 , and compared to glucose content after growth. Cultures were started at an equivalent OD_{600} and glucose was measured once cultures reached an $OD_{600} = 0.1$ (approximately 7 hours of growth, t_7). Cultures of irradiated bacteria were inoculated to a starting OD_{600} equivalent to the starting OD_{600} of the live culture (low), or to the final OD_{600} of 0.1 (high) to account for increases in bioburden occurring in live, dividing culture. Statistical significance analysed by one-way ANOVA (* $P < 0.05$, ** $P < 0.01$, *** $P < 0.001$, **** $P < 0.0001$, n.s. = not significant), data presented as mean \pm SEM ($n = 2$) and indicative of a single experiment.

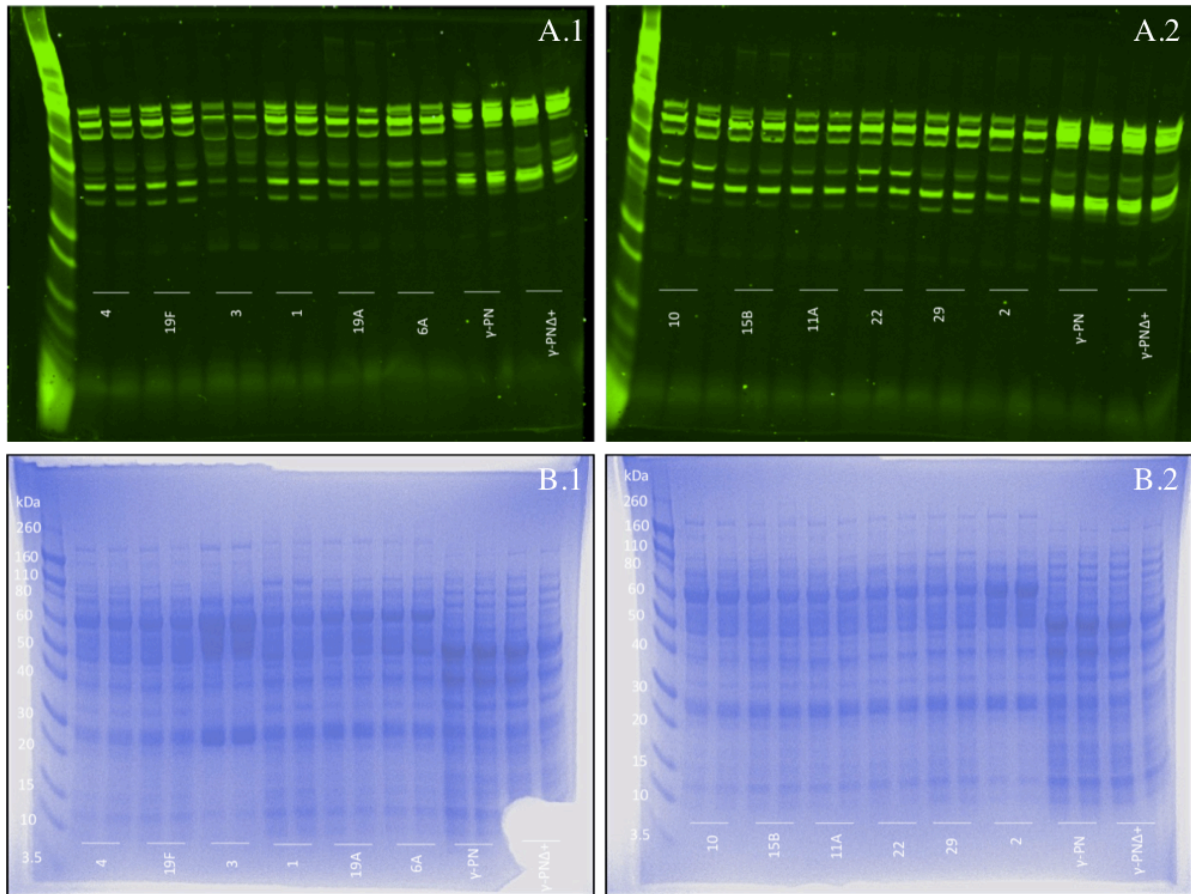


Figure 3.4. Western blot (A) and Coomassie stain (B) of whole-cell lysates from PCV (A.1, B.1) and non-PCV serotypes (A.2, B.2). Live pneumococcal cultures or irradiated vaccine preparations were all lysed by sonication, and 20 μ g of whole cell lysate (determined by BCA protein assay) loaded into wells in duplicate for SDS-PAGE. Separated proteins were transferred to nitrocellulose membranes and probed with serum from Swiss mice vaccinated intramuscularly with alum (A), or stained with Coomassie without transfer to nitrocellulose (B). Bound IgG was detected using IRDye 800CW goat anti-mouse and fluorescence visualised using an Odyssey imaging system. Coomassie staining was visualised using a GelDoc camera.

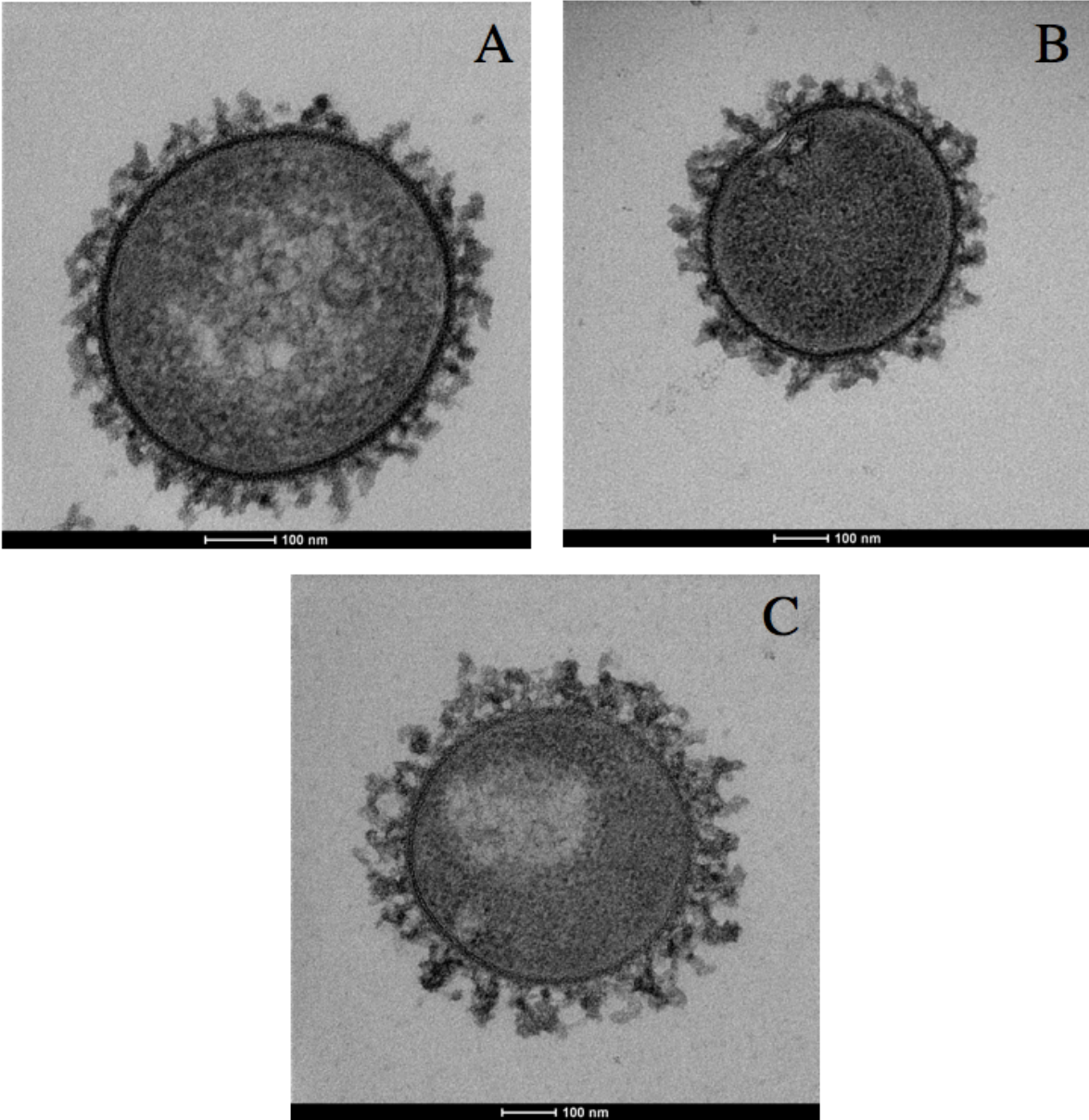


Figure 3.5. Transmission electron microscopy (TEM) of serotype 2 (strain D39) pneumococci grown in different mediums. Pneumococcal cultures were generated by growing D39 in serum broth (A), THY (B), and SILAC + 0.5% glucose (C) to mid-log phase, and capsule structure was visualised using lysine ruthenium red (LRR) fixation. Representative images from each culture are shown and were captured using an FEI Technai G2 Spirit TEM.

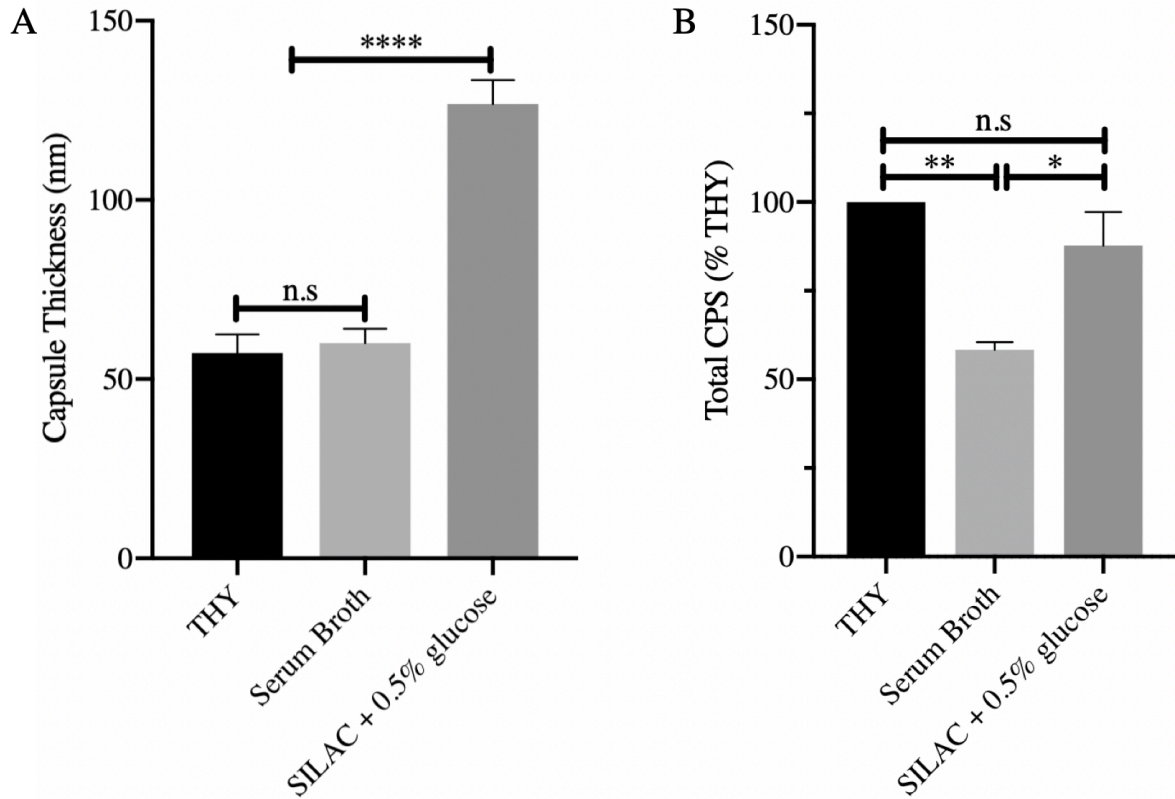


Figure 3.6. Measurements of capsule thickness (A) and total capsular polysaccharide (CPS) production (B) by serotype 2 pneumococci. Capsule thickness was measured using ImageJ software, with measurements taken from a TEM images of pneumococcal cells. Four measurements were taken and averaged to generate a capsule thickness measurement for each cell. Total CPS was measured by uronic acid assay using freshly grown cultures. Growth of all cultures was stopped at mid-log phase. CPS production expressed in terms of CPS produced relative to CPS produced when cells were grown in THY media (% THY). Statistical significance analysed by one-way ANOVA (* $P < 0.05$, ** $P < 0.01$, *** $P < 0.001$, **** $P < 0.0001$, n.s. = not significant), data presented as mean \pm SEM (n = 25/growth condition (A) or 3 (B)) and indicative of a single experiment.

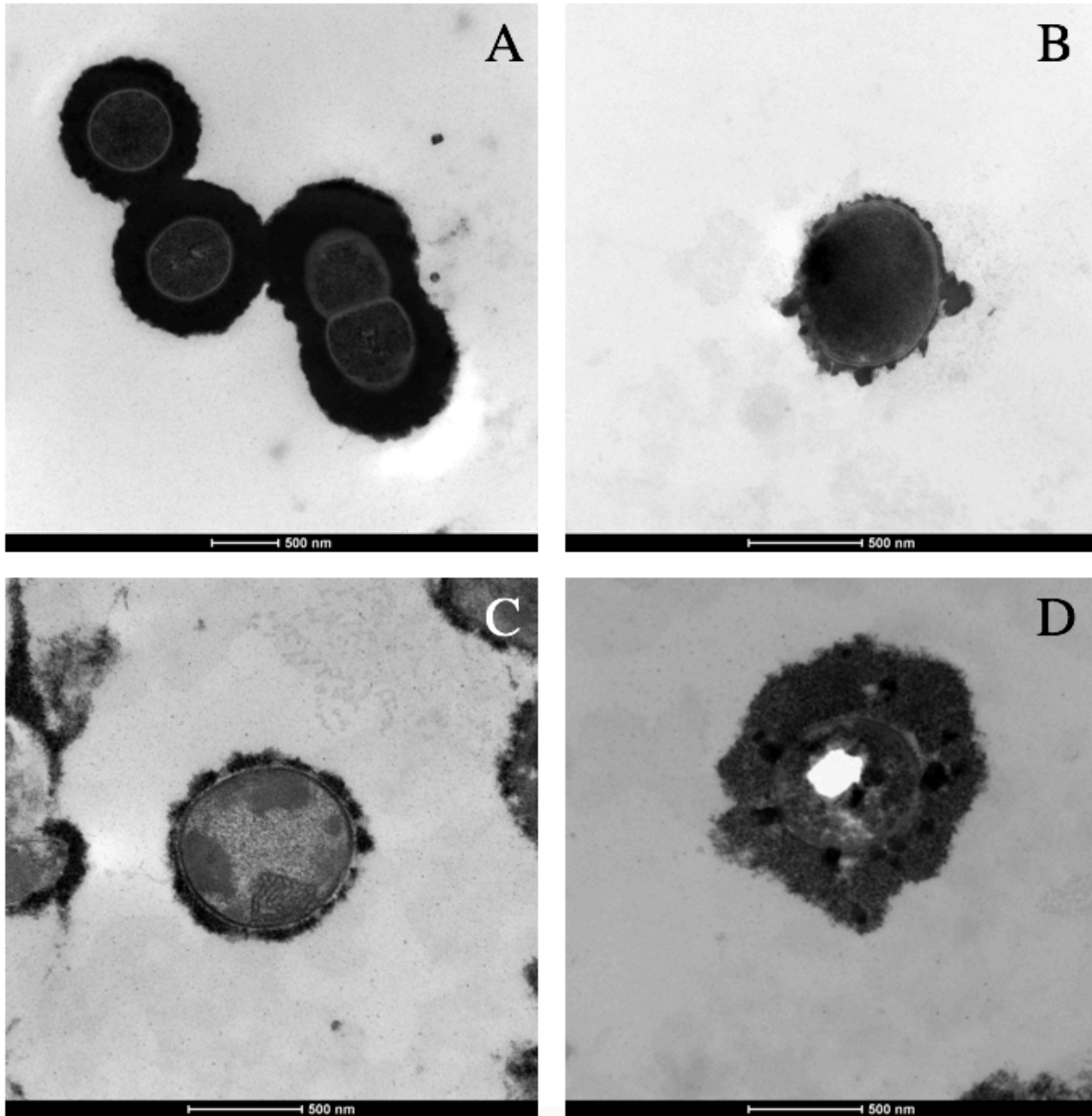


Figure 3.7. Transmission electron microscopy (TEM) of serotype 3 pneumococci grown in different mediums. Pneumococcal cultures were generated by growing serotype 3 in serum broth (A), THY (B), and SILAC + 0.5% glucose (C and D) to equivalent points in the growth curve, and capsule structure was visualised using lysine ruthenium red (LRR) fixation. Representative images from each culture are shown and were captured using an FEI Technai G2 Spirit TEM.

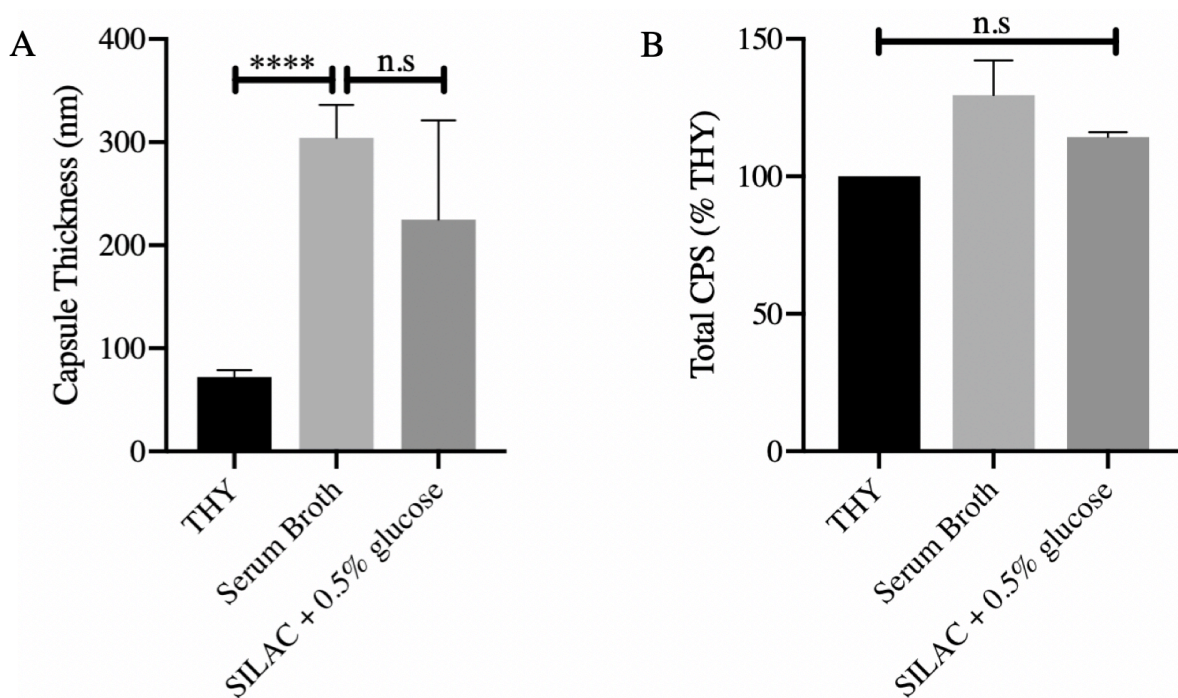


Figure 3.8. Measurements of capsule thickness (A) and total capsular polysaccharide (CPS) production (B) by serotype 3 pneumococci. Capsule thickness was measured using ImageJ software, with measurements taken from a TEM images of pneumococcal cells. Four measurements were taken and averaged to generate a capsule thickness measurement for each cell. Total CPS was measured by uronic acid assay using freshly grown cultures. Growth of all cultures was stopped at mid-log phase. CPS production expressed in terms of CPS produced relative to CPS produced when cells were grown in THY media (% THY). Statistical significance analysed by one-way ANOVA (* $P < 0.05$, ** $P < 0.01$, *** $P < 0.001$, **** $P < 0.0001$, n.s. = not significant), data presented as mean \pm SEM ($n = 25$ /growth condition (A) or 3 (B)) and indicative of a single experiment.

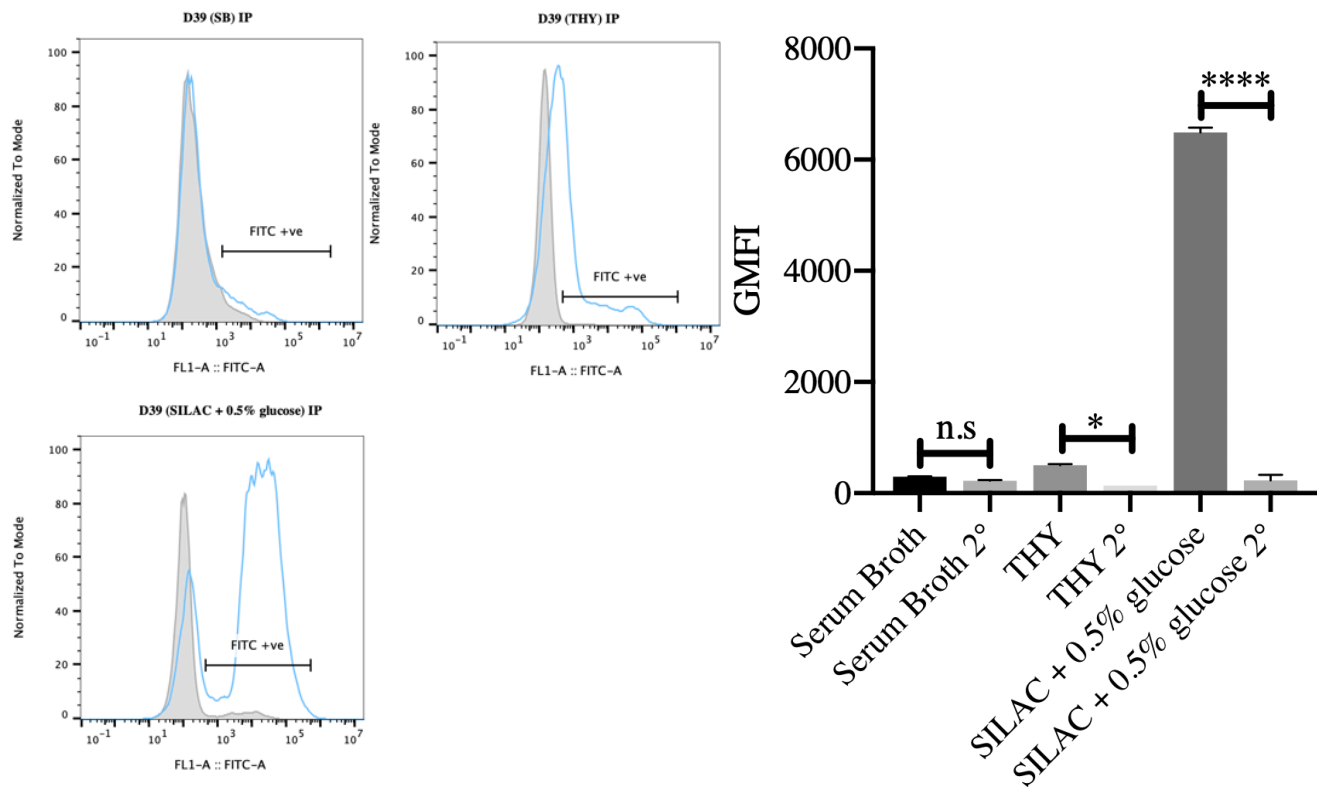


Figure 3.9. IgG binding to serotype 2 pneumococcal cells grown in different mediums and treated with serum from mice vaccinated via IP route. 1×10^7 CFU/well were treated with primary antibody sourced from Swiss mice vaccinated three times intraperitoneally with γ -PN Δ PsaA. Total IgG binding was detected using a FITC-conjugated goat anti-mouse IgG secondary antibody and fluorescence was read using an Accuri flow cytometer. Representative histograms showing shifts in FITC positivity from cells treated with secondary antibody only (grey) to cells also treated with primary antibody (blue line) (left). FITC positive shift quantified for statistical analysis in terms of GMFI (right). Data was analysed by one-way ANOVA by comparing GMFI for primary + secondary antibody treated cells versus GMFI for control cells treated with secondary antibody only (* $P < 0.05$, ** $P < 0.01$, *** $P < 0.001$, **** $P < 0.0001$, n.s. = not significant) and presented as mean \pm SEM (n = 3). Data indicative of a single experiment.

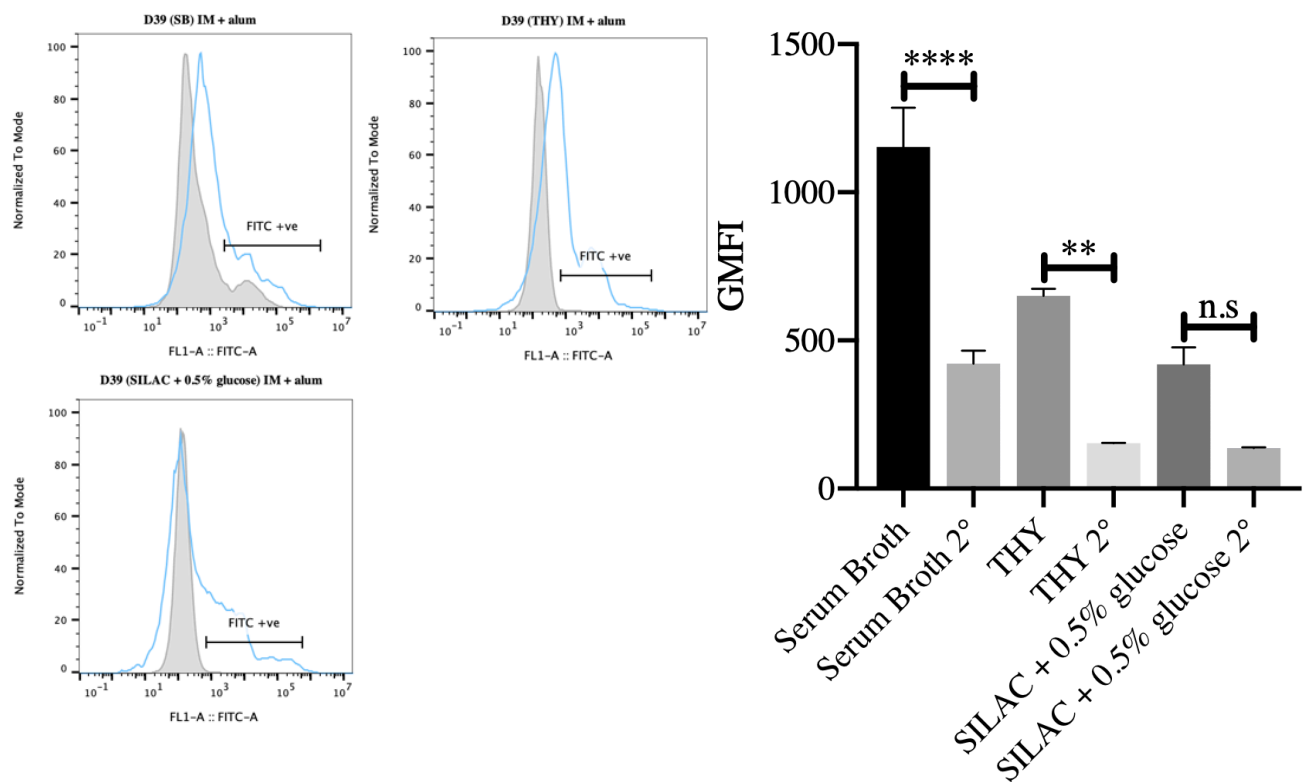


Figure 3.10. IgG binding to serotype 2 pneumococcal cells grown in different mediums and treated with serum from mice vaccinated via IM using alum as adjuvant. 1×10^7 CFU/well were treated with primary antibody sourced from Swiss mice vaccinated three times intramuscularly with γ -PN Δ PsaA and alum. Total IgG binding was detected using a FITC-conjugated goat anti-mouse IgG secondary antibody and fluorescence was read using an Accuri flow cytometer. Representative histograms showing shifts in FITC positivity from cells treated with secondary antibody only (grey) to cells also treated with primary antibody (blue line) (left). FITC positive shift quantified for statistical analysis in terms of GMFI (right). Data was analysed by one-way ANOVA by comparing GMFI for primary + secondary antibody treated cells versus GMFI for control cells treated with secondary antibody only (* $P < 0.05$, ** $P < 0.01$, *** $P < 0.001$, **** $P < 0.0001$, n.s. = not significant) and presented as mean \pm SEM (n = 3). Data indicative of a single experiment.

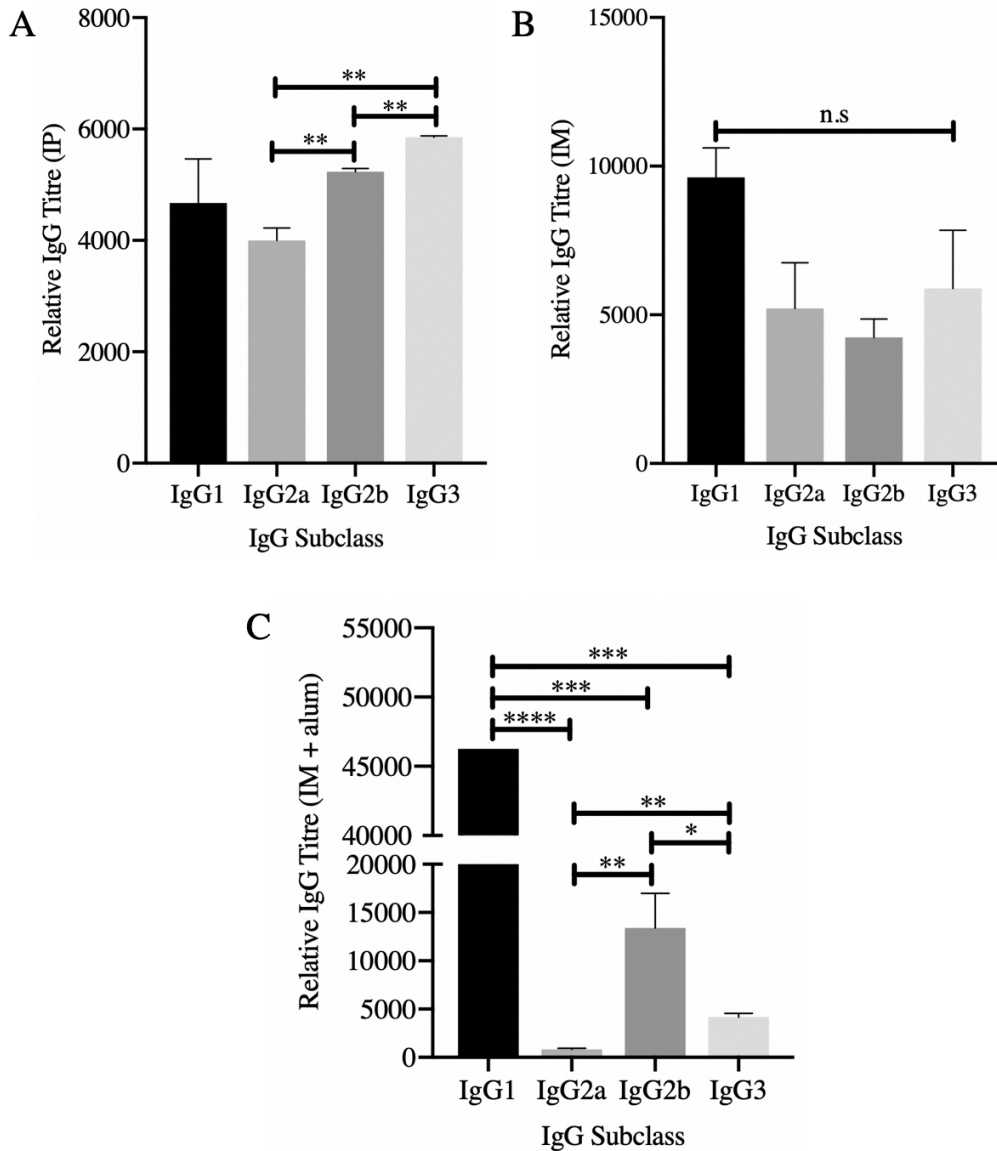


Figure 3.11. The effect of vaccination route and adjuvant on IgG subclass profiles. Swiss mice were vaccinated three times, with doses administered two weeks apart, intraperitoneally (A), intramuscularly (B), or intramuscularly with alum (C) ($n = 6$ per group). Serum was harvested by submandibular bleeding and titres of PN Δ PsaA-specific IgG1, IgG2a, IgG2b, and IgG3 were determined by ELISA. Data presented as mean titres \pm SEM, calculated relative to a cut-off value at 1:160 dilution of control sera from PBS-mock vaccinated mice. Statistical significance analysed by one-way ANOVA (* $P < 0.05$, ** $P < 0.01$, *** $P < 0.001$, **** $P < 0.0001$, n.s. = not significant). Data indicative of a single experiment.

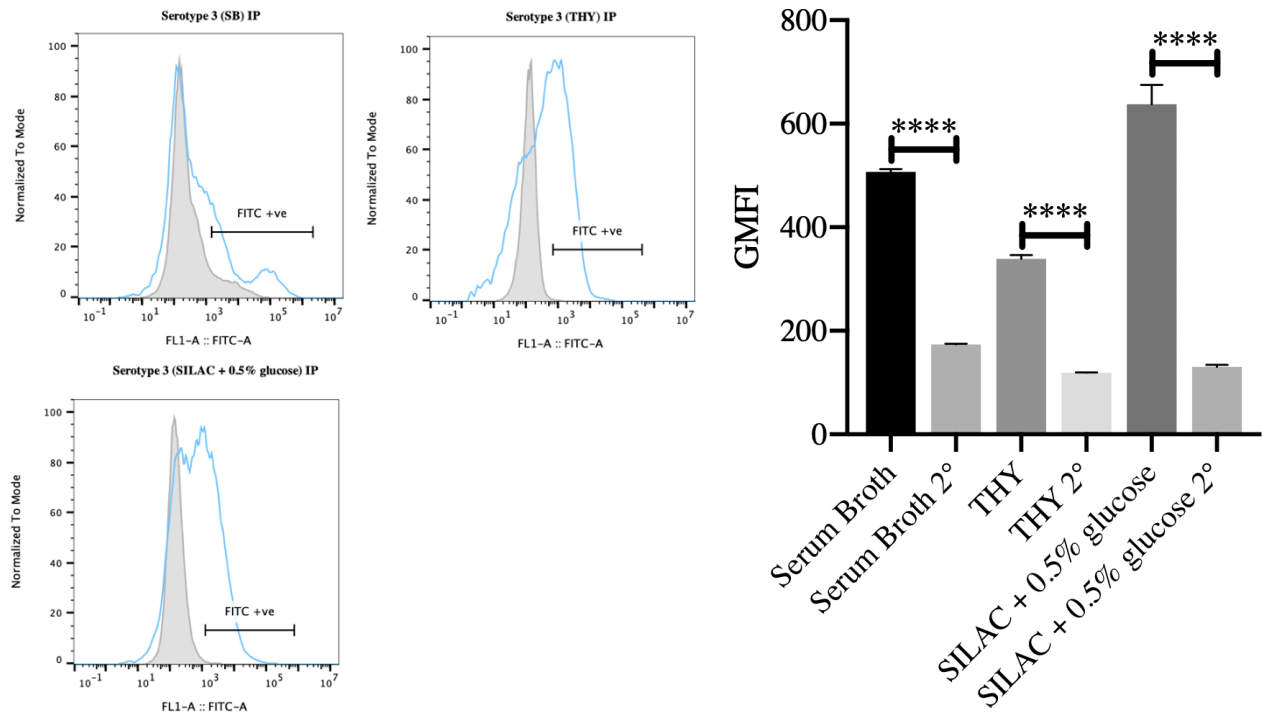


Figure 3.12. IgG binding to serotype 3 pneumococcal cells grown in different mediums and treated with serum from mice vaccinated via IP route. 1×10^7 CFU/well were treated with primary antibody sourced from Swiss mice vaccinated three times intraperitoneally with γ -PN Δ PsaA. Total IgG binding was detected using a FITC-conjugated goat anti-mouse IgG secondary antibody and fluorescence was read using an Accuri flow cytometer. Representative histograms showing shifts in FITC positivity from cells treated with secondary antibody only (grey) to cells also treated with primary antibody (blue line) (left). FITC positive shift quantified for statistical analysis in terms of GMFI (right). Data was analysed by one-way ANOVA by comparing primary antibody treated GMFI to secondary only GMFI (* $P < 0.05$, ** $P < 0.01$, *** $P < 0.001$, **** $P < 0.0001$, n.s. = not significant) and presented as mean \pm SEM (n = 3). Data indicative of a single experiment.

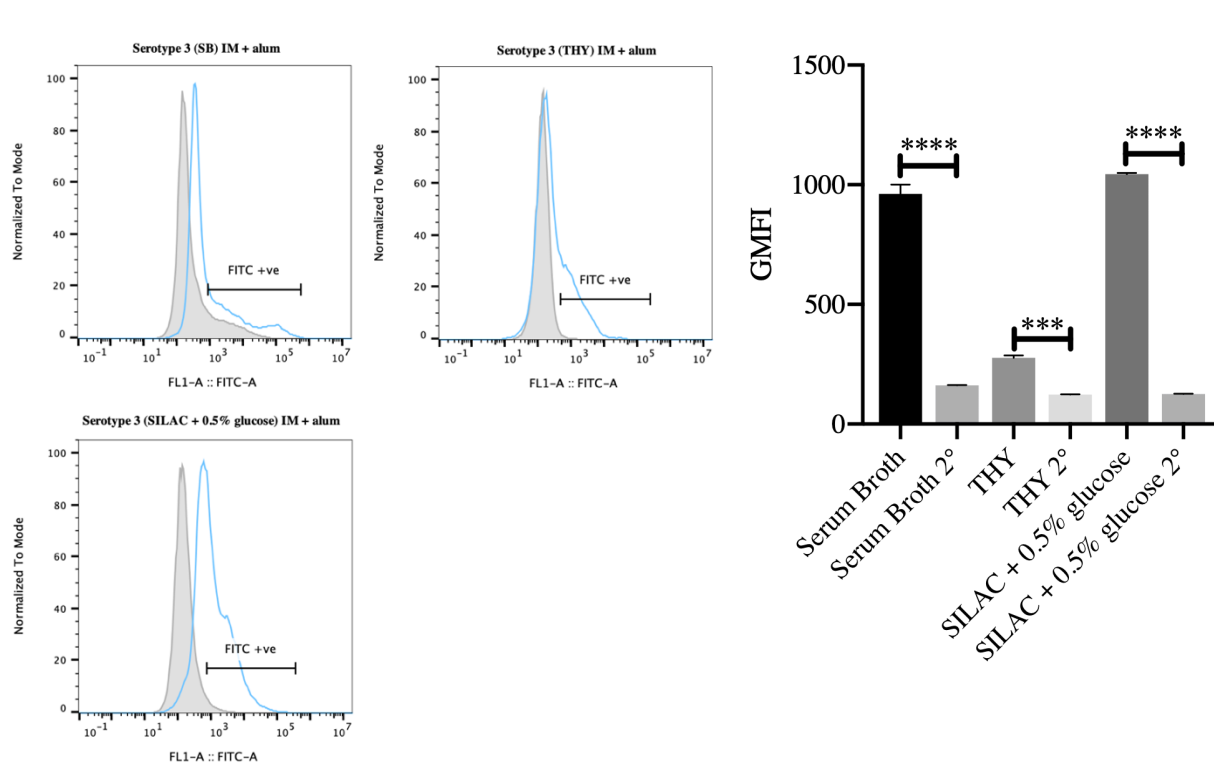


Figure 3.13. IgG binding to serotype 3 pneumococcal cells grown in different mediums and treated with serum from mice vaccinated via IM route with alum adjuvant. 1×10^7 CFU/well were treated with primary antibody sourced from Swiss mice vaccinated three times intramuscularly with γ -PN Δ PsaA and alum. Total IgG binding was detected using a FITC-conjugated goat anti-mouse IgG secondary antibody and fluorescence was read using an Accuri flow cytometer. Representative histograms showing shifts in FITC positivity from cells treated with secondary antibody only (grey) to cells also treated with primary antibody (blue line) (left). FITC positive shift quantified for statistical analysis in terms of GMFI (right). Data was analysed by one-way ANOVA by comparing primary antibody treated GMFI to secondary only GMFI (* $P < 0.05$, ** $P < 0.01$, *** $P < 0.001$, **** $P < 0.0001$, n.s. = not significant) and presented as mean \pm SEM (n = 3). Data indicative of a single experiment.

CHAPTER 4

Discussion

4.1. Characterisation of gamma-irradiated pneumococci

While gamma-irradiated whole-cell vaccines are yet to be tested clinically, this technology has received considerable attention in the laboratory setting and has been proposed as a method to generate a non-dividing but metabolically active (NDMA) cells that can be used as highly immunogenic vaccines. However, the metabolic and enzymatic activities of NDMA-like organisms are yet to be fully characterised. Thus, I examined the retention of specific enzymatic, replicative, and metabolic activities related to gamma-irradiated pneumococcal vaccine γ -PN Δ PsaA to generate a more in-depth picture of the high immunogenicity and the serotype-independent protective immunity reported previously by our lab. Furthermore, this characterisation also serves to assess whether gamma-irradiated pneumococci can be considered NDMA organisms, or if a new classification is required.

Firstly, I examined the neuraminidase activity of live pneumococci, compared to bacteria inactivated using gamma irradiation, heat, and ethanol. These inactivation techniques have been previously used in laboratory settings to generate whole-cell bacterial antigens [129, 155]. As anticipated, live pneumococci possessed the highest level of neuraminidase activity in this assay. Importantly, while irradiated pneumococci showed a significant drop in enzymatic activity compared to this live counterpart, I detected significant levels of neuraminidase activity for the irradiated materials compared to heat or ethanol inactivated preparations. The drop on enzymatic activity for irradiated materials compared to the live control is likely due to some damage to protein antigens sustained during the irradiation process via the generation of oxidising free radicals. Damage caused by oxidising free radicals is classified as a mechanism of ‘indirect’ damage’ during the process of irradiation. While possible damage to proteins cannot be avoided during the irradiation process, damage can be mitigated through modification of irradiation conditions. Previously, our group have employed the use of dry-ice to minimise damage to vaccine antigens, reducing both the formation and the movement of free radicals generated during the irradiation process [156, 157]. Conversely, damage mitigation against specific targets, such as proteins, cannot be employed when broad-target methods such as heat and ethanol are used as inactivation methods. As a result, irradiated

pneumococci possessed significantly higher neuraminidase activity relative to heat- and ethanol-killed pneumococci.

In fact, these more conventional inactivation methods reduced enzymatic activity to almost undetectable levels. In fact, one of the primary mechanisms by which heat-killing inactivates biological organisms is through the denaturation of proteins, preventing enzymatic and metabolic activities required for viability [158]. Thus, it was unsurprising to observe that no neuraminidase activity was retained by heat-killed pneumococci. Interestingly, very limited neuraminidase activity was retained by ethanol-killed pneumococci, though this was significantly lower than activity possessed by gamma-irradiated pneumococci. As ethanol-killed cultures were checked for sterility, these results are likely not due to the presence of viable bacteria in the killed culture. Exposure to ethanol denatures proteins through the disruption of hydrophobic interactions [159]. This may be a concentration- or time-dependent process, and thus increases in the concentration of ethanol or exposure time may lead to different results.

In addition to neuraminidase activity, I assessed the maintenance of transcriptional activities by irradiated pneumococci. In order to assess the production of new RNA transcripts, I examined transcription from inducible genes. The inducible genes chosen, *aga*, *rafK*, *rafG*, and *galK* are controlled by the raffinose and galactose operons, respectively. Raffinose and galactose act as alternative carbon sources for the pneumococcus, utilised when the preferred carbon source, glucose, is unavailable. These experiments aimed to test whether irradiated pneumococci possess transcriptional activities, subsequently indicating that another enzyme, RNA polymerase, remained active after irradiation. Indirectly, this would also demonstrate that irradiated pneumococci retain functional sugar import enzymes and are also capable of responding to new environmental signals.

These data revealed a number of insights into genomic damage sustained via gamma irradiation that may warrant further investigation. Gamma irradiation results in the introduction of breakages into genetic material, known as direct damage. The points at which gamma-rays interact with the genome and introduce breakages is random, however, it appears that some

regions of the genome may be more susceptible to direct damage than others. In the case of *aga* and *galK* expression, irradiated pneumococci produced fewer transcripts overall, but this was not a significant decrease when compared with live pneumococci exposed to the same inducing conditions. This trend towards lower rates of transcription is likely a result of some bacteria in the 10^{10} CFU/ml population sustaining damage to the genes of interest. Interestingly, this trend was not consistent in the four genes examined as my data demonstrated significantly reduced rates of transcription for *rafK* and *rafG* genes in irradiated pneumococci under inducing conditions. It is possible that variations in expression level may have arisen due to differences in gene sizes, with longer genomic regions sustaining damage more frequently than a smaller counterpart. However, this possibility could be ruled out considering the fact that *aga* is the largest gene of the four assayed (2160bp), and *galK*, *rafK*, and *rafG* are of similar sizes (1179bp, 1131bp, 839bp, respectively). Alternatively, as both genes exhibited significantly reduced expression belonged to the raffinose operon, it is possible that raffinose import may be affected by treatment with gamma-irradiation. However, this is unlikely to be the cause for the variation in gene expression as *aga* expression was not similarly affected. Therefore, the physical characteristics of coding regions or control elements may play a role in enhanced susceptibility to direct damage by gamma rays. Characteristics that may warrant further investigation include examining whether epigenetic changes can modify susceptibility to direct damage. It is reasonable to expect that changes in susceptibility may be partially due to differences in DNA conformation, with tightly packed genetic material less likely to sustain damage compared to coding regions with a looser conformation. Other aspects that may warrant investigation include examining whether specific inducer or repressor proteins are associated with both genes that demonstrated significant decreases in transcriptional levels, with enhanced sensitivity possibly associated with protein rather than DNA damage.

In addition to investigating gene expression, I examined the retention of metabolic activity in terms of glucose utilisation. Depletion of glucose from growth media after a period of seven hours was used as an indicator of metabolism. As anticipated, glucose content was significantly depleted after seven hours when live pneumococci were incubated under replicative conditions. Comparatively, no significant depletion in glucose was detected when irradiated pneumococci were cultured under the same conditions. The observed lack of glucose depletion

over time could be due to the low bacterial burden in the culture when irradiated bacteria were inoculated to an equivalent starting OD to their live counterpart, as irradiated pneumococci do not replicate. To account for this possibility, the culture of irradiated pneumococci was set up to an OD value equivalent to that of the live pneumococcal culture at the end of the growth period. Interestingly, incubating the irradiated culture with a high OD value had no impact on glucose utilisation over the course of the incubation period, with these conditions similarly resulting in no depletion of glucose. There are a number of possibilities that can potentially explain this observation. Firstly, irradiated pneumococci may take up an amount of glucose required for normal metabolism, however, due to their inability to divide, metabolic products create an internal backlog, shutting down further metabolism via feedback loops. Secondly, the enzymes of irradiated pneumococci may not remain active for extended periods of time after cultures are thawed, preventing the detection of early metabolic activity under less sensitive conditions. Finally, cell lysis may occur over time due to damage accrued throughout the irradiation process, which would deplete the number of bacteria available to take up glucose, and also release internalised glucose back into the growth media. Overall, this assay indicates that irradiated bacteria are not broadly metabolically active, despite possessing functional enzymes.

4.2. Interactions between γ -PN Δ PsaA-induced antibodies and encapsulated strains of pneumococci

As our γ -PN Δ PsaA vaccine was designed to induce an immune response against highly conserved sub-capsular antigens, I examined the breadth of serotype cross-reactivity of vaccine-induced antibodies. 13vPCV and non-PCV serotypes were included in my screening panel. Overall, γ -PN Δ PsaA-induced antibodies were shown to be capable of recognising an array of protein antigens expressed by all serotypes examined. A high degree of consistency in terms of banding patterns was observed between each lysate, attesting to the highly conserved nature of these sub-capsular antigens. Banding intensity appeared to be the most consistent across all serotypes for higher kDa bands, with more variability in banding intensity existing at mid- to low-kDa ranges. Changes in banding intensity between serotypes may be due to

differential expression as some antigens, such as PspA, exhibit serological variability (as discussed in Chapter 1). As our vaccine antigen is a derivative of serotype 2, expression of antigens such as PspA from different serological families may result in changes in banding patterns relative to the homologous serotype 2 lysate. Despite the possible presence of antigenic variability between each serotype, the induction of an antibody response against all surface antigens ensures that cross-reactivity is maintained through redundancy; while antibodies might react poorly against a specific antigen, the multi-valent nature of our whole-cell vaccine ensures that an antibody response exists against other surface antigens to accommodate for some serological mismatch.

In addition to examining vaccine-induced immune sera cross-reactivity to whole cell lysates from different serotypes, I investigated antibody binding to whole-cell encapsulated pneumococci. This is essential to gain insight into the action of antibodies in a more clinically relevant setting, as pneumococcal disease is mainly caused by encapsulated strains of bacteria. Considering that the pneumococcus is known to vary capsule expression *in vivo*, I grew pneumococci using different culture conditions in an attempt to manipulate capsule expression to examine how the capsule hinders access to sub-capsular antigens, and which stage of infection vaccine-induced antibodies may be targeting. Capsule structure was assessed both in terms of width and overall polysaccharide production. Interestingly, I found that cultures expressing larger capsules in terms of polysaccharide length do not necessarily express the highest levels of total polysaccharide. Bacterial growth in serum broth and THY media generated capsules of equivalent thicknesses, while growth in SILAC + 0.5% glucose medium produced much larger capsules. Despite similarities in size, cultures of THY grown serotype 2 cells expressed more total polysaccharide than their serum broth grown counterparts. Most interestingly, despite SILAC + 0.5% glucose grown D39 expressing a significantly larger capsule than both THY and serum broth grown D39, cultures grown under these conditions produced total CPS concentrations equivalent to those produced by THY grown cultures. These results indicate that growth conditions influence capsule production not only in terms of thickness, but also in terms of overall structure. For example, comparing serum broth and THY grown cells indicates that while the polysaccharide chains detected for both cultures may be of a similar length, THY grown cells may decorate their surfaces with more chains than their

serum broth grown counterparts. Contrastingly, SILAC + 0.5% grown D39 appears to generate long polysaccharide chains, though these must decorate the bacterial surface more sparsely, leading to equivalence in total CPS production with THY grown cells.

To examine whether these trends were a serotype-independent phenomenon, I also examined capsule expression by serotype 3 cells grown under the same conditions. Interestingly, the trends observed in serotype 2 cultures was not repeated when using serotype 3, indicating that responses to changes in growth media are serotype dependent. Under each condition, serotype 3 capsules were measured to be significantly thicker than their serotype 2 counterparts, with growth in serum broth rather than SILAC + 0.5% glucose producing the largest capsule. Additionally, unlike serotype 2, there appeared to be no significant difference in total polysaccharide content in each culture despite large differences in capsule size. When TEM and UAA data are taken together, this may suggest that cells grown in serum broth possess a more homogenous capsule structure than those grown in THY. When grown in serum broth, polysaccharide chains appear to uniformly decorate the cell surface, while cells grown in THY appear to possess a mixture of long and short polysaccharide chains organised into nodule-like structures or coating the surface evenly.

In order to examine the impact of encapsulation on antibody binding, I firstly examined IgG binding to serotype 2 cells grown under different conditions. For this study, I used immune sera from mice vaccinated using different route of administration to address whether vaccination route can influence IgG subclass profiles and antibody-pathogen interactions. I firstly examined IgG binding to serotype 2 pneumococci using serum from mice vaccinated using IP administration route. Interestingly, while serum broth and THY grown cells expressed relatively thin capsules, IgG binding to these cells was not significantly different, or only increased mildly, when compared to their secondary antibody only controls. Comparatively, SILAC + 0.5% glucose grown cells, which exhibited a thick capsule, showed a substantial increase in IgG binding compared to both its control and either counterpart. Taken together with data from the TEM and Uronic Acid Assay (UAA) experiments, this may indicate that capsule thickness alone is not always indicative of the degree of efficacy of sub-capsular antigen shielding by the capsule. Additionally, structural aspects of how polysaccharide chains

are arranged on the bacterial surface must also be considered. In this case, while growth in SILAC + 0.5% glucose may lead to the production of long polysaccharide chains and thus a thick capsule, the overall content of capsular polysaccharide indicated by UAA suggests a sparsely encapsulated phenotype, a phenotype what can be characterised accurately based on TEM images alone.

In order to examine the impact of encapsulation in a more clinically relevant setting, I repeated this experiment using serum from mice vaccinated IM, with alum included in vaccine formulation as an adjuvant. Interestingly, the trends observed using immune sera from IP vaccinated mice could not be repeated using sera from IM vaccinated mice. While THY grown cells showed mid-range IgG binding once more, IgG binding trends in serum broth and SILAC + 0.5% glucose grown cells was reversed. A factor associated with the serum may influence IgG binding to encapsulated pneumococci and therefore I examined IgG subclass profiles. In the case of sera generated using IP vaccination, there is no clear domination by a single subclass, with relative IgG1, IgG2b, and IgG3 titres slightly higher than relative IgG2a titres. Comparatively, serum from mice vaccinated via the IM route with alum as adjuvant is clearly dominated by the IgG1 subclass, followed by IgG2b with significantly lower relative titres, IgG3, and finally IgG2a. This is typical of an antibody response induced in the presence of alum, which favours the generation of a Th2-type response dominated by the IgG1 subclass [160, 161]. While this profile of IgG subclasses is associated with higher IgG binding to serum broth grown D39, the binding to SILAC + 0.5% glucose grown D39 is much lower than that observed for immune sera from mice vaccinated via IP route, with GMFI values of ~1200 and ~6500, respectively. This may suggest that this subclass profile offers sub-optimal IgG binding against encapsulated pneumococci, particularly since Th2-type responses are most closely associated with immunity against helminth-type pathogens [162].

Subsequently, I examined IgG binding to serotype 3 pneumococcal cells using immune sera from mice vaccinated via IP route and mice vaccinated via IM with alum as an adjuvant. Overall, rates of IgG binding were lower against serotype 3 cells treated with IP serum when compared to cells treated with serum from mice vaccinated using IM route with alum. In each case, however, higher levels of IgG binding were not polarised towards cells grown in one

particular growth medium. IgG binding tended to be slightly higher against SILAC + 0.5% grown cells, with IgG binding to serum broth cells closely behind. Similar to the serotype 2, IgG binding to serotype 3 was lowest against THY grown cells when using either serum type. As serotype 3 cells typically expressed thicker capsules than their serotype 2 counterparts under all growth conditions, these capsular phenotypes may be more effective at preventing IgG binding, hence the lower GMFI values observed against all serotype 3 cells relative to serotype 2. Combining antibody binding data may suggest that immune serum generated by vaccination using IM with alum as an adjuvant (dominated by IgG1) is better able to bind to pneumococci with a broader range of capsule thicknesses, and hence is potentially better able to bypass the capsule for effective protein antigen binding. Conversely, immune sera from mice vaccinated using IP route of administration (equal distribution of IgG subclasses) was more effective in binding to pneumococcal cells when SILAC + 0.5% glucose was used for growth. The sparser capsule generated by culture in this media type only may allow binding by the 'non-optimal' IgG profile associated with IP immunisation.

Taken together, these data indicate that aspects associated with both capsule phenotype and serum subclass profiles can influence IgG binding to encapsulated pneumococcal cells. The functional relevance of these IgG binding rates remains of particular interest. For example, there may be a specific subclass that binds pneumococci with any capsular phenotype most consistently. It may also be worth examining whether higher rates of IgG binding correlate with increased OPK, or if there is a minimum level of IgG binding required for protection against pneumococcal disease.

4.3. Future directions

A key characteristic shared by both KBMA and NDMA organisms lies in their ability to combine the safety of killed vaccines with the enhanced immunogenicity of live-attenuated vaccines. Both KBMA and NDMA organisms have been demonstrated to stimulate immune responses comparable to those induced in mice following non-lethal challenge with the live organism. This characteristic is thought to be due to the maintenance of metabolic activities. Traditionally, the retention of translational activities has acted as a benchmark for deeming

whole-cell antigens as KBMA or NDMA. To complete the examination of our whole-cell antigen, radiolabelled amino acid incorporation may be utilised to examine whether protein synthesis pathways similarly remain functional. Furthermore, it would be of interest to examine whether the gamma-irradiated preparation stimulates immune signalling to a comparable degree with its live counterpart. Innate immune signalling may be examined *in vitro* by comparing TLR stimulation by irradiated and live vaccine preparations, while adaptive responses may be further examined via administration of a sub-lethal dose of live pneumococci or γ -PN Δ PsaA. Of further interest may be examining which processes are required for enhanced immune signalling by the inactivated organism. For example, immune signalling experiments could be repeated to compare signalling via γ -PN Δ PsaA alone, and γ -PN Δ PsaA treated with a transcription inhibitor to see if mRNA production is responsible for enhanced signalling by irradiated organisms versus those inactivated using methods such as heat or ethanol.

Further examination of IgG binding to encapsulated pneumococci will be required if an ideal IgG subclass profile is to be elucidated. Rather than examining total IgG binding, future experiments may focus on examining whether there is a specific IgG subclass that is most effective at binding sub-capsular antigens. This may be achieved through flow cytometry analysis using secondary antibodies specific to each IgG subclass, rather than to total IgG. Additionally, my data showed that immune sera from mice vaccinated via the IM route with alum adjuvant was capable of binding pneumococci expressing a variety of capsular phenotypes, albeit at lower levels than immune serum from mice vaccinated via the IP route. It would be beneficial to examine whether these lower levels of IgG binding are associated with efficient OPK activity. This can be achieved *in vitro* using a phagocytic cell line and spot plating to generate OPKA titres.

4.4. Conclusion

To date, the only pneumococcal vaccines available on the market consist of purified polysaccharide capsule alone (PPV), or conjugated to a protein carrier (PCV). While effective against the limited number of serotypes included in their formulation, the PPV and PCV pneumococcal vaccines suffer from a shared shortcoming; serotype specificity. To address this

issue, our lab has endeavoured to develop a new, serotype-independent pneumococcal vaccine using unencapsulated whole cells inactivated using gamma-irradiation. Our formulation branches away from traditional pneumococcal vaccines, containing a whole-cell inactivated antigen rather than purified pneumococcal components. The removal of the polysaccharide capsule further subverts characteristics of conventional pneumococcal vaccines, leading to the induction of a B cell-dependent immune response specific to highly conserved sub-capsular antigens, conferring the serotype-independent nature of our vaccine.

Overall, this study has further characterised irradiated pneumococcal cells. I have demonstrated that these inactivated cells retain enzymatic activities both externally (neuraminidase) and internally (RNA polymerase). Furthermore, my data represent the first illustration that irradiated bacteria are capable of responding to environmental signals in terms of available carbohydrates, and can modifying gene expression accordingly. These experiments also provided further insight into how gene structure may influence susceptibility to damage by gamma-irradiation. Our vaccine preparation does not appear to retain activities associated with carbohydrate utilisation and metabolism in a broader sense. This may not preclude irradiated pneumococci from being classed as an NDMA organism, however. While metabolic activity reported by Brockstedt and colleagues, and Magnani and colleagues was established by demonstrating translational pathways remain active, the detection of microbial viability and enhanced immunogenicity is thought to occur via sensing of microbial mRNA [143, 144]. Therefore, the demonstration of new mRNA synthesis may be a more appropriate benchmark for the classification of organisms as NDMA, as illustrated for gamma-irradiated *S. pneumoniae*, unless long-term protein synthesis can be demonstrated as this would also require the synthesis of new mRNA transcripts.

Additionally, I have shown that capsular phenotype can be influenced by changes in growth conditions that may impact both polysaccharide chain length and density on the bacterial surface. These experiments subsequently revealed that polysaccharide chain length alone is not necessarily an ideal indicator of sub-capsular antigen shielding capabilities. Furthermore, IgG binding to pneumococcal cells is also impacted by the IgG subclass profiles induced by different routes of vaccination. Taken together this data provides valuable insight into the

characteristics of a gamma-irradiated pneumococcal vaccine that will help us to understand the high immunogenicity and the serotype-independent protection induced by this vaccine candidate.

CHAPTER 5

References

1. van Rossum, A.M.C., Lysenko, E. S., Weiser, J. N., *Host and Bacterial Factors Contributing to the Clearance of Colonization by Streptococcus pneumoniae in a Murine Model*. Infect Immun, 2005. **73**(11): p. 7718 - 7726.
2. Habib, M., B.D. Porter, and C. Satzke, *Capsular serotyping of Streptococcus pneumoniae using the Quellung reaction*. J Vis Exp, 2014(84): p. e51208.
3. Bridy-Pappas, A.E., et al., *Streptococcus pneumoniae: description of the pathogen, disease epidemiology, treatment, and prevention*. Pharmacotherapy, 2005. **25**(9): p. 1193-212.
4. Kadioglu, A., et al., *The role of Streptococcus pneumoniae virulence factors in host respiratory colonization and disease*. Nat Rev Microbiol, 2008. **6**(4): p. 288-301.
5. Morens, D.M., J.K. Taubenberger, and A.S. Fauci, *Predominant role of bacterial pneumonia as a cause of death in pandemic influenza: implications for pandemic influenza preparedness*. J Infect Dis, 2008. **198**(7): p. 962-70.
6. Verma, R. and P. Khanna, *Pneumococcal conjugate vaccine: a newer vaccine available in India*. Hum Vaccin Immunother, 2012. **8**(9): p. 1317-20.
7. Harboe, Z.B., et al., *Temporal trends in invasive pneumococcal disease and pneumococcal serotypes over 7 decades*. Clin Infect Dis, 2010. **50**(3): p. 329-37.
8. Fedson, D.S. and J.A. Scott, *The burden of pneumococcal disease among adults in developed and developing countries: what is and is not known*. Vaccine, 1999. **17 Suppl 1**: p. S11-8.
9. Bliss, S.J., et al., *The evidence for using conjugate vaccines to protect HIV-infected children against pneumococcal disease*. Lancet Infect Dis, 2008. **8**(1): p. 67-80.
10. Grabowska, K., et al., *Occurrence of invasive pneumococcal disease and number of excess cases due to influenza*. BMC Infect Dis, 2006. **6**: p. 58.
11. O'Brien, K.L., et al., *Severe pneumococcal pneumonia in previously healthy children: the role of preceding influenza infection*. Clin Infect Dis, 2000. **30**(5): p. 784-9.
12. Kadioglu, A., et al., *Host cellular immune response to pneumococcal lung infection in mice*. Infect Immun, 2000. **68**(2): p. 492-501.
13. Bogaert, D., R. De Groot, and P.W. Hermans, *Streptococcus pneumoniae colonisation: the key to pneumococcal disease*. Lancet Infect Dis, 2004. **4**(3): p. 144-54.
14. Schuchat, A., et al., *Bacterial meningitis in the United States in 1995*. Active Surveillance Team. N Engl J Med, 1997. **337**(14): p. 970-6.
15. Bijlsma, M.W., et al., *Community-acquired bacterial meningitis in adults in the Netherlands, 2006-14: a prospective cohort study*. Lancet Infect Dis, 2016. **16**(3): p. 339-47.
16. Goetghebuer, T., et al., *Outcome of meningitis caused by Streptococcus pneumoniae and Haemophilus influenzae type b in children in The Gambia*. Trop Med Int Health, 2000. **5**(3): p. 207-13.
17. Muhe, L. and K.P. Klugman, *Pneumococcal and Haemophilus influenzae meningitis in a children's hospital in Ethiopia: serotypes and susceptibility patterns*. Trop Med Int Health, 1999. **4**(6): p. 421-7.
18. Koedel, U., W.M. Scheld, and H.W. Pfister, *Pathogenesis and pathophysiology of pneumococcal meningitis*. Lancet Infect Dis, 2002. **2**(12): p. 721-36.

19. *Global Pneumococcal Disease and Vaccine*. 2018. Available from: <https://www.cdc.gov/pneumococcal/global.html>.
20. Collaborators, G.B.D.L.R.I., *Estimates of the global, regional, and national morbidity, mortality, and aetiologies of lower respiratory infections in 195 countries, 1990-2016: a systematic analysis for the Global Burden of Disease Study 2016*. *Lancet Infect Dis*, 2018. **18**(11): p. 1191-1210.
21. Fine, M.J., et al., *Prognosis and outcomes of patients with community-acquired pneumonia. A meta-analysis*. *JAMA*, 1996. **275**(2): p. 134-41.
22. Tan, T.Q., et al., *Clinical characteristics of children with complicated pneumonia caused by Streptococcus pneumoniae*. *Pediatrics*, 2002. **110**(1 Pt 1): p. 1-6.
23. van der Poll, T. and S.M. Opal, *Pathogenesis, treatment, and prevention of pneumococcal pneumonia*. *Lancet*, 2009. **374**(9700): p. 1543-56.
24. Swiatlo, E., et al., *Contribution of choline-binding proteins to cell surface properties of Streptococcus pneumoniae*. *Infect Immun*, 2002. **70**(1): p. 412-5.
25. Rosenow, C., et al., *Contribution of novel choline-binding proteins to adherence, colonization and immunogenicity of Streptococcus pneumoniae*. *Mol Microbiol*, 1997. **25**(5): p. 819-29.
26. Hammerschmidt, S., *Adherence molecules of pathogenic pneumococci*. *Curr Opin Microbiol*, 2006. **9**(1): p. 12-20.
27. Camara, M., et al., *A neuraminidase from Streptococcus pneumoniae has the features of a surface protein*. *Infect Immun*, 1994. **62**(9): p. 3688-95.
28. Elm, C., et al., *Ectodomains 3 and 4 of human polymeric Immunoglobulin receptor (hplgR) mediate invasion of Streptococcus pneumoniae into the epithelium*. *J Biol Chem*, 2004. **279**(8): p. 6296-304.
29. Kim, J.O., et al., *Relationship between cell surface carbohydrates and intrastain variation on opsonophagocytosis of Streptococcus pneumoniae*. *Infect Immun*, 1999. **67**(5): p. 2327-33.
30. Nelson, A.L., et al., *Capsule enhances pneumococcal colonization by limiting mucus-mediated clearance*. *Infect Immun*, 2007. **75**(1): p. 83-90.
31. Xayarath, B. and J. Yother, *Mutations blocking side chain assembly, polymerization, or transport of a Wzy-dependent Streptococcus pneumoniae capsule are lethal in the absence of suppressor mutations and can affect polymer transfer to the cell wall*. *J Bacteriol*, 2007. **189**(9): p. 3369-81.
32. Calix, J.J., et al., *Biochemical, genetic, and serological characterization of two capsule subtypes among Streptococcus pneumoniae Serotype 20 strains: discovery of a new pneumococcal serotype*. *J Biol Chem*, 2012. **287**(33): p. 27885-94.
33. Geno, K.A., et al., *Pneumococcal Capsules and Their Types: Past, Present, and Future*. *Clin Microbiol Rev*, 2015. **28**(3): p. 871-99.
34. Kolkman, M.A., et al., *The capsule polysaccharide synthesis locus of streptococcus pneumoniae serotype 14: Identification of the glycosyl transferase gene cps14E*. *J Bacteriol*, 1996. **178**(13): p. 3736-41.
35. Forsee, W.T., R.T. Cartee, and J. Yother, *Biosynthesis of type 3 capsular polysaccharide in Streptococcus pneumoniae. Enzymatic chain release by an abortive translocation process*. *J Biol Chem*, 2000. **275**(34): p. 25972-8.

36. Weinberger, D.M., et al., *Pneumococcal capsular polysaccharide structure predicts serotype prevalence*. PLoS Pathog, 2009. **5**(6): p. e1000476.
37. Hausdorff, W.P., D.R. Feikin, and K.P. Klugman, *Epidemiological differences among pneumococcal serotypes*. Lancet Infect Dis, 2005. **5**(2): p. 83-93.
38. Brady, A.M., et al., *Low invasiveness of pneumococcal serotype 11A is linked to ficolin-2 recognition of O-acetylated capsule epitopes and lectin complement pathway activation*. J Infect Dis, 2014. **210**(7): p. 1155-65.
39. Kelly, T., J.P. Dillard, and J. Yother, *Effect of genetic switching of capsular type on virulence of Streptococcus pneumoniae*. Infect Immun, 1994. **62**(5): p. 1813-9.
40. Tuomanen, E.I. and H.R. Masure, *Molecular and cellular biology of pneumococcal infection*. Microb Drug Resist, 1997. **3**(4): p. 297-308.
41. Geng, J.G., et al., *Neutrophil recognition requires a Ca(2+)-induced conformational change in the lectin domain of GMP-140*. J Biol Chem, 1991. **266**(33): p. 22313-8.
42. Cundell, D.R., et al., *Streptococcus pneumoniae anchor to activated human cells by the receptor for platelet-activating factor*. Nature, 1995. **377**(6548): p. 435-8.
43. Mogensen, T.H., et al., *Live Streptococcus pneumoniae, Haemophilus influenzae, and Neisseria meningitidis activate the inflammatory response through Toll-like receptors 2, 4, and 9 in species-specific patterns*. J Leukoc Biol, 2006. **80**(2): p. 267-77.
44. Yoshimura, A., et al., *Cutting edge: recognition of Gram-positive bacterial cell wall components by the innate immune system occurs via Toll-like receptor 2*. J Immunol, 1999. **163**(1): p. 1-5.
45. Dessing, M.C., et al., *Role played by Toll-like receptors 2 and 4 in lipoteichoic acid-induced lung inflammation and coagulation*. J Infect Dis, 2008. **197**(2): p. 245-52.
46. Knapp, S., et al., *Toll-like receptor 2 plays a role in the early inflammatory response to murine pneumococcal pneumonia but does not contribute to antibacterial defense*. J Immunol, 2004. **172**(5): p. 3132-8.
47. Echchannaoui, H., et al., *Toll-like receptor 2-deficient mice are highly susceptible to Streptococcus pneumoniae meningitis because of reduced bacterial clearing and enhanced inflammation*. J Infect Dis, 2002. **186**(6): p. 798-806.
48. Malley, R., et al., *Recognition of pneumolysin by Toll-like receptor 4 confers resistance to pneumococcal infection*. Proc Natl Acad Sci U S A, 2003. **100**(4): p. 1966-71.
49. McNeela, E.A., et al., *Pneumolysin activates the NLRP3 inflammasome and promotes proinflammatory cytokines independently of TLR4*. PLoS Pathog, 2010. **6**(11): p. e1001191.
50. Klein, M., et al., *Innate immunity to pneumococcal infection of the central nervous system depends on toll-like receptor (TLR) 2 and TLR4*. J Infect Dis, 2008. **198**(7): p. 1028-36.
51. Hemmi, H., et al., *A Toll-like receptor recognizes bacterial DNA*. Nature, 2000. **408**(6813): p. 740-5.
52. Albiger, B., et al., *Toll-like receptor 9 acts at an early stage in host defence against pneumococcal infection*. Cell Microbiol, 2007. **9**(3): p. 633-44.

53. Gordon, S.B., et al., *Intracellular trafficking and killing of Streptococcus pneumoniae by human alveolar macrophages are influenced by opsonins*. *Infect Immun*, 2000. **68**(4): p. 2286-93.
54. Brown, J.S., et al., *The classical pathway is the dominant complement pathway required for innate immunity to Streptococcus pneumoniae infection in mice*. *Proc Natl Acad Sci U S A*, 2002. **99**(26): p. 16969-74.
55. Walport, M.J., *Complement. First of two parts*. *N Engl J Med*, 2001. **344**(14): p. 1058-66.
56. Clas, F. and M. Loos, *Antibody-independent binding of the first component of complement (C1) and its subcomponent C1q to the S and R forms of Salmonella minnesota*. *Infect Immun*, 1981. **31**(3): p. 1138-44.
57. Feinstein, A., N. Richardson, and M.I. Taussig, *Immunoglobulin flexibility in complement activation*. *Immunol Today*, 1986. **7**(6): p. 169-74.
58. Kaplan, M.H. and J.E. Volanakis, *Interaction of C-reactive protein complexes with the complement system. I. Consumption of human complement associated with the reaction of C-reactive protein with pneumococcal C-polysaccharide and with the choline phosphatides, lecithin and sphingomyelin*. *J Immunol*, 1974. **112**(6): p. 2135-47.
59. Hyams, C., et al., *The Streptococcus pneumoniae capsule inhibits complement activity and neutrophil phagocytosis by multiple mechanisms*. *Infect Immun*, 2010. **78**(2): p. 704-15.
60. Hammerschmidt, S., et al., *Illustration of pneumococcal polysaccharide capsule during adherence and invasion of epithelial cells*. *Infect Immun*, 2005. **73**(8): p. 4653-67.
61. Brinkmann, V., et al., *Neutrophil extracellular traps kill bacteria*. *Science*, 2004. **303**(5663): p. 1532-5.
62. Beiter, K., et al., *An endonuclease allows Streptococcus pneumoniae to escape from neutrophil extracellular traps*. *Curr Biol*, 2006. **16**(4): p. 401-7.
63. Roche, A.M., et al., *Antibody blocks acquisition of bacterial colonization through agglutination*. *Mucosal Immunol*, 2015. **8**(1): p. 176-85.
64. Nakasone, C., Yamamoto, N., Nakamatsu, M., Kinjo, T., Miyagi, K., Uezu, K., Nakamura, K., Higa, F., Ishikawa, H., O'brien, R. L., Ikuta, K., Kaku, M., Fujita, J., Kawakami, K., *Accumulation of gamma/delta T cells in the lungs and their roles in neutrophil-mediated host defense against pneumococcal infection*. *Microbes and Infection*, 2007. **9**(3): p. 251-258.
65. Lockhart, E., A.M. Green, and J.L. Flynn, *IL-17 production is dominated by gamma delta T cells rather than CD4 T cells during Mycobacterium tuberculosis infection*. *Journal of Immunology*, 2006. **177**(7): p. 4662-4669.
66. Babb, R., et al., *Intranasal vaccination with gamma-irradiated Streptococcus pneumoniae whole-cell vaccine provides serotype-independent protection mediated by B-cells and innate IL-17 responses*. *Clinical Science*, 2016. **130**(9): p. 697-710.
67. Kolls, J.K. and A. Linden, *Interleukin-17 family members and inflammation*. *Immunity*, 2004. **21**(4): p. 467-476.

68. Dworkin, M.S., et al., *Pneumococcal disease among human immunodeficiency virus-infected persons: incidence, risk factors, and impact of vaccination*. Clin Infect Dis, 2001. **32**(5): p. 794-800.
69. Gill, C.J., et al., *Impact of human immunodeficiency virus infection on Streptococcus pneumoniae colonization and seroepidemiology among Zambian women*. J Infect Dis, 2008. **197**(7): p. 1000-5.
70. Roche, A.M., S.J. King, and J.N. Weiser, *Live attenuated Streptococcus pneumoniae strains induce serotype-independent mucosal and systemic protection in mice*. Infect Immun, 2007. **75**(5): p. 2469-75.
71. Malley, R., et al., *CD4+ T cells mediate antibody-independent acquired immunity to pneumococcal colonization*. Proc Natl Acad Sci U S A, 2005. **102**(13): p. 4848-53.
72. Lu, Y.J., et al., *Interleukin-17A mediates acquired immunity to pneumococcal colonization*. PLoS Pathog, 2008. **4**(9): p. e1000159.
73. Zhang, Z., T.B. Clarke, and J.N. Weiser, *Cellular effectors mediating Th17-dependent clearance of pneumococcal colonization in mice*. J Clin Invest, 2009. **119**(7): p. 1899-909.
74. Wright, A.K., et al., *Experimental human pneumococcal carriage augments IL-17A-dependent T-cell defence of the lung*. PLoS Pathog, 2013. **9**(3): p. e1003274.
75. Nakada, T.A., et al., *IL17A genetic variation is associated with altered susceptibility to Gram-positive infection and mortality of severe sepsis*. Crit Care, 2011. **15**(5): p. R254.
76. Chen, J., et al., *The polymorphism of IL-17 G-152A was associated with childhood asthma and bacterial colonization of the hypopharynx in bronchiolitis*. J Clin Immunol, 2010. **30**(4): p. 539-45.
77. Wilson, R., et al., *Protection against Streptococcus pneumoniae lung infection after nasopharyngeal colonization requires both humoral and cellular immune responses*. Mucosal Immunol, 2015. **8**(3): p. 627-39.
78. Cohen, J.M., et al., *Protective contributions against invasive Streptococcus pneumoniae pneumonia of antibody and Th17-cell responses to nasopharyngeal colonisation*. PLoS One, 2011. **6**(10): p. e25558.
79. Roche, A.M. and J.N. Weiser, *Identification of the targets of cross-reactive antibodies induced by Streptococcus pneumoniae colonization*. Infect Immun, 2010. **78**(5): p. 2231-9.
80. Colino, J., Y. Shen, and C.M. Snapper, *Dendritic cells pulsed with intact Streptococcus pneumoniae elicit both protein- and polysaccharide-specific immunoglobulin isotype responses in vivo through distinct mechanisms*. J Exp Med, 2002. **195**(1): p. 1-13.
81. AlonsoDeVelasco, E., et al., *Streptococcus pneumoniae: virulence factors, pathogenesis, and vaccines*. Microbiol Rev, 1995. **59**(4): p. 591-603.
82. Anttila, M., et al., *Contribution of serotype-specific IgG concentration, IgG subclasses and relative antibody avidity to opsonophagocytic activity against Streptococcus pneumoniae*. Clin Exp Immunol, 1999. **118**(3): p. 402-7.
83. Lortan, J.E., A.S. Kaniuk, and M.A. Monteil, *Relationship of in vitro phagocytosis of serotype 14 Streptococcus pneumoniae to specific class and IgG subclass antibody levels in healthy adults*. Clin Exp Immunol, 1993. **91**(1): p. 54-7.

84. Wilson, R., et al., *Naturally Acquired Human Immunity to Pneumococcus Is Dependent on Antibody to Protein Antigens*. PLoS Pathog, 2017. **13**(1): p. e1006137.
85. Robinson, K.A., et al., *Epidemiology of invasive Streptococcus pneumoniae infections in the United States, 1995-1998: Opportunities for prevention in the conjugate vaccine era*. JAMA, 2001. **285**(13): p. 1729-35.
86. Turner, P., et al., *Serum antibody responses to pneumococcal colonization in the first 2 years of life: results from an SE Asian longitudinal cohort study*. Clin Microbiol Infect, 2013. **19**(12): p. E551-8.
87. Laine, C., et al., *Age-specific immunoglobulin g (IgG) and IgA to pneumococcal protein antigens in a population in coastal kenya*. Infect Immun, 2004. **72**(6): p. 3331-5.
88. Holmlund, E., et al., *Development of natural antibodies to pneumococcal surface protein A, pneumococcal surface adhesin A and pneumolysin in Filipino pregnant women and their infants in relation to pneumococcal carriage*. Vaccine, 2006. **24**(1): p. 57-65.
89. Rapola, S., et al., *Natural development of antibodies to pneumococcal surface protein A, pneumococcal surface adhesin A, and pneumolysin in relation to pneumococcal carriage and acute otitis media*. J Infect Dis, 2000. **182**(4): p. 1146-52.
90. McCool, T.L., et al., *The immune response to pneumococcal proteins during experimental human carriage*. J Exp Med, 2002. **195**(3): p. 359-65.
91. Mulholland, K., *Strategies for the control of pneumococcal diseases*. Vaccine, 1999. **17**: p. S79-S84.
92. Grimwood, K., et al., *Antibiotic management of pneumococcal infections in an era of increased resistance*. J Paediatr Child Health, 1997. **33**(4): p. 287-95.
93. Klugman, K.P., *Pneumococcal resistance to antibiotics*. Clin Microbiol Rev, 1990. **3**(2): p. 171-96.
94. Miranda Novales, M.G., et al., *Streptococcus pneumoniae: low frequency of penicillin resistance and high resistance to trimethoprim-sulfamethoxazole in nasopharyngeal isolates from children in a rural area in Mexico*. Arch Med Res, 1997. **28**(4): p. 559-63.
95. Huovinen, P., *Resistance to trimethoprim-sulfamethoxazole*. Clin Infect Dis, 2001. **32**(11): p. 1608-14.
96. Black, S., et al., *Efficacy, safety and immunogenicity of heptavalent pneumococcal conjugate vaccine in children. Northern California Kaiser Permanente Vaccine Study Center Group*. Pediatr Infect Dis J, 2000. **19**(3): p. 187-95.
97. Whitney, C.G., et al., *Decline in invasive pneumococcal disease after the introduction of protein-polysaccharide conjugate vaccine*. N Engl J Med, 2003. **348**(18): p. 1737-46.
98. *Pneumovax 23*. Australian Immunisation Handbook 2018; Available from: <https://immunisationhandbook.health.gov.au/vaccines/pneumovax-23>.
99. *Pneumococcal Disease*. 2019; Available from: <https://immunisationhandbook.health.gov.au/vaccine-preventable-diseases/pneumococcal-disease>.

100. Snapper, C.M. and J.J. Mond, *A model for induction of T cell-independent humoral immunity in response to polysaccharide antigens*. J Immunol, 1996. **157**(6): p. 2229-33.
101. Poland, G.A., *The burden of pneumococcal disease: the role of conjugate vaccines*. Vaccine, 1999. **17**(13-14): p. 1674-9.
102. Jackson, L.A., et al., *Effectiveness of pneumococcal polysaccharide vaccine in older adults*. N Engl J Med, 2003. **348**(18): p. 1747-55.
103. Ortqvist, A., et al., *Randomised trial of 23-valent pneumococcal capsular polysaccharide vaccine in prevention of pneumonia in middle-aged and elderly people*. Swedish Pneumococcal Vaccination Study Group. Lancet, 1998. **351**(9100): p. 399-403.
104. Rubins, J.B., et al., *Determination of antibody responses of elderly adults to all 23 capsular polysaccharides after pneumococcal vaccination*. Infect Immun, 1999. **67**(11): p. 5979-84.
105. Wuorimaa, T. and H. Kayhty, *Current state of pneumococcal vaccines*. Scand J Immunol, 2002. **56**(2): p. 111-29.
106. Ben-Shimol, S., et al., *Near-elimination of otitis media caused by 13-valent pneumococcal conjugate vaccine (PCV) serotypes in southern Israel shortly after sequential introduction of 7-valent/13-valent PCV*. Clin Infect Dis, 2014. **59**(12): p. 1724-32.
107. Lexau, C.A., et al., *Changing epidemiology of invasive pneumococcal disease among older adults in the era of pediatric pneumococcal conjugate vaccine*. JAMA, 2005. **294**(16): p. 2043-51.
108. Weinberger, D.M., R. Malley, and M. Lipsitch, *Serotype replacement in disease after pneumococcal vaccination*. Lancet, 2011. **378**(9807): p. 1962-73.
109. Obaro, S.K., et al., *Carriage of pneumococci after pneumococcal vaccination*. Lancet, 1996. **348**(9022): p. 271-2.
110. Mbelle, N., et al., *Immunogenicity and impact on nasopharyngeal carriage of a nonavalent pneumococcal conjugate vaccine*. J Infect Dis, 1999. **180**(4): p. 1171-6.
111. van Gils, E.J., et al., *Effect of reduced-dose schedules with 7-valent pneumococcal conjugate vaccine on nasopharyngeal pneumococcal carriage in children: a randomized controlled trial*. JAMA, 2009. **302**(2): p. 159-67.
112. Lipsitch, M., et al., *Strain characteristics of Streptococcus pneumoniae carriage and invasive disease isolates during a cluster-randomized clinical trial of the 7-valent pneumococcal conjugate vaccine*. J Infect Dis, 2007. **196**(8): p. 1221-7.
113. Miller, E., et al., *Herd immunity and serotype replacement 4 years after seven-valent pneumococcal conjugate vaccination in England and Wales: an observational cohort study*. Lancet Infect Dis, 2011. **11**(10): p. 760-8.
114. Hicks, L.A., et al., *Incidence of pneumococcal disease due to non-pneumococcal conjugate vaccine (PCV7) serotypes in the United States during the era of widespread PCV7 vaccination, 1998-2004*. J Infect Dis, 2007. **196**(9): p. 1346-54.
115. Brueggemann, A.B., et al., *Temporal and geographic stability of the serogroup-specific invasive disease potential of Streptococcus pneumoniae in children*. J Infect Dis, 2004. **190**(7): p. 1203-11.

116. Carvalho, M.G., et al., *Confirmation of nontypeable Streptococcus pneumoniae-like organisms isolated from outbreaks of epidemic conjunctivitis as Streptococcus pneumoniae*. J Clin Microbiol, 2003. **41**(9): p. 4415-7.
117. Xu, Q., et al., *Nontypeable Streptococcus pneumoniae as an otopathogen*. Diagn Microbiol Infect Dis, 2011. **69**(2): p. 200-4.
118. Lacapa, R., et al., *Changing epidemiology of invasive pneumococcal disease among White Mountain Apache persons in the era of the pneumococcal conjugate vaccine*. Clin Infect Dis, 2008. **47**(4): p. 476-84.
119. Briles, D.E., J. Yother, and L.S. McDaniel, *Role of pneumococcal surface protein A in the virulence of Streptococcus pneumoniae*. Rev Infect Dis, 1988. **10 Suppl 2**: p. S372-4.
120. Shaper, M., et al., *PspA protects Streptococcus pneumoniae from killing by apolactoferrin, and antibody to PspA enhances killing of pneumococci by apolactoferrin [corrected]*. Infect Immun, 2004. **72**(9): p. 5031-40.
121. McDaniel, L.S., et al., *PspA, a surface protein of Streptococcus pneumoniae, is capable of eliciting protection against pneumococci of more than one capsular type*. Infect Immun, 1991. **59**(1): p. 222-8.
122. Wu, H.Y., et al., *Intranasal immunization of mice with PspA (pneumococcal surface protein A) can prevent intranasal carriage, pulmonary infection, and sepsis with Streptococcus pneumoniae*. J Infect Dis, 1997. **175**(4): p. 839-46.
123. Briles, D.E., et al., *The potential to use PspA and other pneumococcal proteins to elicit protection against pneumococcal infection*. Vaccine, 2000. **18**(16): p. 1707-11.
124. Sampson, J.S., et al., *Limited diversity of Streptococcus pneumoniae psaA among pneumococcal vaccine serotypes*. Infect Immun, 1997. **65**(5): p. 1967-71.
125. Dintilhac, A., et al., *Competence and virulence of Streptococcus pneumoniae: Adc and PsaA mutants exhibit a requirement for Zn and Mn resulting from inactivation of putative ABC metal permeases*. Mol Microbiol, 1997. **25**(4): p. 727-39.
126. Johnson, S.E., et al., *Inhibition of pneumococcal carriage in mice by subcutaneous immunization with peptides from the common surface protein pneumococcal surface adhesin a*. J Infect Dis, 2002. **185**(4): p. 489-96.
127. Alexander, J.E., et al., *Immunization of mice with pneumolysin toxoid confers a significant degree of protection against at least nine serotypes of Streptococcus pneumoniae*. Infect Immun, 1994. **62**(12): p. 5683-8.
128. Ogunniyi, A.D., et al., *Development of a vaccine against invasive pneumococcal disease based on combinations of virulence proteins of Streptococcus pneumoniae*. Infect Immun, 2007. **75**(1): p. 350-7.
129. Lu, Y.J., et al., *Options for inactivation, adjuvant, and route of topical administration of a killed, unencapsulated pneumococcal whole-cell vaccine*. Clin Vaccine Immunol, 2010. **17**(6): p. 1005-12.
130. Malley, R., et al., *Intranasal immunization with killed unencapsulated whole cells prevents colonization and invasive disease by capsulated pneumococci*. Infect Immun, 2001. **69**(8): p. 4870-3.

131. Hogenesch, H., et al., *Formulation of a killed whole cell pneumococcus vaccine - effect of aluminum adjuvants on the antibody and IL-17 response*. J Immune Based Ther Vaccines, 2011. **9**: p. 5.
132. Goncalves, V.M., et al., *Development of a whole cell pneumococcal vaccine: BPL inactivation, cGMP production, and stability*. Vaccine, 2014. **32**(9): p. 1113-20.
133. Lu, Y.J., et al., *GMP-grade pneumococcal whole-cell vaccine injected subcutaneously protects mice from nasopharyngeal colonization and fatal aspiration-sepsis*. Vaccine, 2010. **28**(47): p. 7468-75.
134. Jacobs, G.P., *A review of the effects of gamma radiation on pharmaceutical materials*. J Biomater Appl, 1995. **10**(1): p. 59-96.
135. Farkas, J., *Irradiation as a method for decontaminating food. A review*. Int J Food Microbiol, 1998. **44**(3): p. 189-204.
136. Elliott, L.H., J.B. McCormick, and K.M. Johnson, *Inactivation of Lassa, Marburg, and Ebola viruses by gamma irradiation*. J Clin Microbiol, 1982. **16**(4): p. 704-8.
137. Grieb, T., et al., *Effective use of gamma irradiation for pathogen inactivation of monoclonal antibody preparations*. Biologicals, 2002. **30**(3): p. 207-216.
138. Sommer, R., et al., *Inactivation of bacteriophages in water by means of non-ionizing (UV-253.7 nm) and ionizing (gamma) radiation: A comparative approach*. Water Research, 2001. **35**(13): p. 3109-3116.
139. Kitchen, A.D., et al., *Effect of gamma irradiation on the human immunodeficiency virus and human coagulation proteins*. Vox Sang, 1989. **56**(4): p. 223-9.
140. Alsharifi, M. and A. Mullbacher, *The gamma-irradiated influenza vaccine and the prospect of producing safe vaccines in general*. Immunol Cell Biol, 2010. **88**(2): p. 103-4.
141. Sander, L.E., *Improved vaccines through targeted manipulation of the body's immunological risk-assessment?* Bioessays, 2012. **34**(10): p. 876-84.
142. Blander, J.M. and L.E. Sander, *Beyond pattern recognition: five immune checkpoints for scaling the microbial threat*. Nat Rev Immunol, 2012. **12**(3): p. 215-25.
143. Mourao-Sa, D., S. Roy, and J.M. Blander, *Vita-PAMPs: signatures of microbial viability*. Adv Exp Med Biol, 2013. **785**: p. 1-8.
144. Sander, L.E., et al., *Detection of prokaryotic mRNA signifies microbial viability and promotes immunity*. Nature, 2011. **474**(7351): p. 385-9.
145. Brockstedt, D.G., et al., *Killed but metabolically active microbes: a new vaccine paradigm for eliciting effector T-cell responses and protective immunity*. Nat Med, 2005. **11**(8): p. 853-60.
146. Magnani, D.M., et al., *Nondividing but metabolically active gamma-irradiated Brucella melitensis is protective against virulent B. melitensis challenge in mice*. Infect Immun, 2009. **77**(11): p. 5181-9.
147. Dubensky, T.W., Jr., et al., *Killed but metabolically active vaccines*. Curr Opin Biotechnol, 2012. **23**(6): p. 917-23.
148. Bickle, Q.D., et al., *Immunization of mice with gamma-irradiated intramuscularly injected schistosomula of Schistosoma mansoni*. Parasitology, 1979. **79**(2): p. 209-22.
149. Reitman, M., H.R. Tribble, Jr., and L. Green, *Gamma-irradiated Venezuelan equine encephalitis vaccines*. Appl Microbiol, 1970. **19**(5): p. 763-7.

150. Mellouk, S., et al., *Protection against malaria induced by irradiated sporozoites*. Lancet, 1990. **335**(8691): p. 721.
151. Soiffer, R., et al., *Vaccination with irradiated autologous melanoma cells engineered to secrete human granulocyte-macrophage colony-stimulating factor generates potent antitumor immunity in patients with metastatic melanoma*. Proc Natl Acad Sci U S A, 1998. **95**(22): p. 13141-6.
152. Choi, E., et al., *First Phase I human clinical trial of a killed whole-HIV-1 vaccine: demonstration of its safety and enhancement of anti-HIV antibody responses*. Retrovirology, 2016. **13**(1): p. 82.
153. Alsharifi, M., et al., *Intranasal flu vaccine protective against seasonal and H5N1 avian influenza infections*. PLoS One, 2009. **4**(4): p. e5336.
154. Shahrudin, S., et al., *Gamma-irradiated rotavirus: A possible whole virus inactivated vaccine*. PLoS One, 2018. **13**(6): p. e0198182.
155. Mills, K.H., et al., *Cell-mediated immunity to Bordetella pertussis: role of Th1 cells in bacterial clearance in a murine respiratory infection model*. Infect Immun, 1993. **61**(2): p. 399-410.
156. Jordan, R.T. and L.L. Kempe, *Inactivation of some animal viruses with gamma radiation from cobalt-60*. Proc Soc Exp Biol Med, 1956. **91**(2): p. 212-5.
157. David, S.C., et al., *The effect of gamma-irradiation conditions on the immunogenicity of whole-inactivated Influenza A virus vaccine*. Vaccine, 2017. **35**(7): p. 1071-1079.
158. Mackey, B.M., et al., *Thermal denaturation of whole cells and cell components of Escherichia coli examined by differential scanning calorimetry*. J Gen Microbiol, 1991. **137**(10): p. 2361-74.
159. Piper, P.W., *The heat shock and ethanol stress responses of yeast exhibit extensive similarity and functional overlap*. FEMS Microbiology Letters, 1995. **134**: p. 121 - 127.
160. Kool, M., K. Fierens, and B.N. Lambrecht, *Alum adjuvant: some of the tricks of the oldest adjuvant*. J Med Microbiol, 2012. **61**(Pt 7): p. 927-34.
161. Mawas, F., I.M. Feavers, and M.J. Corbel, *Serotype of Streptococcus pneumoniae capsular polysaccharide can modify the Th1/Th2 cytokine profile and IgG subclass response to pneumococcal-CRM(197) conjugate vaccines in a murine model*. Vaccine, 2000. **19**(9-10): p. 1159-66.
162. D'Elia, M.M., et al., *T-cell response to bacterial agents*. J Infect Dev Ctries, 2011. **5**(9): p. 640-5.